# Non-linear effects

## Yannis PAPAPHILIPPOU
### Accelerator and Beam Physics group
### Beams Department
### CERN

**Joint University Accelerator School**

Archamps, FRANCE

22-24 January 2014

- **Resonances and the path to chaos**
  - ❑ Topology of 3$^{rd}$ and 4$^{th}$ order resonance
  - ❑ Path to chaos and resonance overlap
  - ❑ Dynamic aperture simulations
- **Frequency map analysis**
  - ❑ NAFF algorithm
  - ❑ Aspects of frequency maps
  - ❑ Frequency and diffusion maps for the LHC
  - ❑ Frequency map for lepton rings
  - ❑ Working point choice
  - ❑ Beam-beam effect
- **Experiments**
  - ❑ Experimental frequency maps
  - ❑ Beam loss frequency maps
  - ❑ Space-charge frequency scan

- **Resonances and the path to chaos**
  - Topology of 3$^{rd}$ and 4$^{th}$ order resonance
  - Path to chaos and resonance overlap
  - Dynamic aperture simulations
- Frequency map analysis
  - NAFF algorithm
  - Aspects of frequency maps
  - Frequency and diffusion maps for the LHC
  - Frequency map for lepton rings
  - Working point choice
  - Beam-beam effect
- Experiments
  - Experimental frequency maps
  - Beam loss frequency maps
  - Space-charge frequency scan

- Record the particle coordinates at one location (BPM)
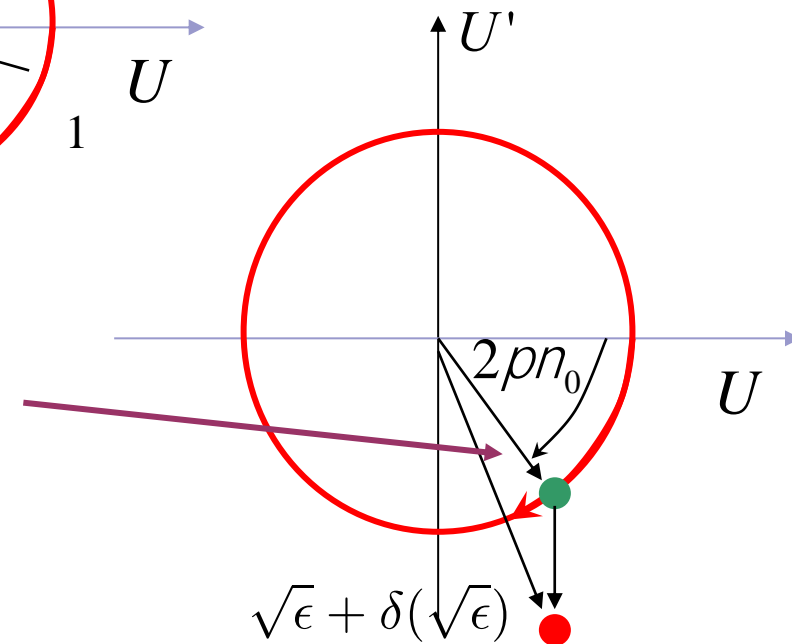- Unperturbed motion lies on a circle in normalized coordinates (simple rotation)

Poincaré Section:
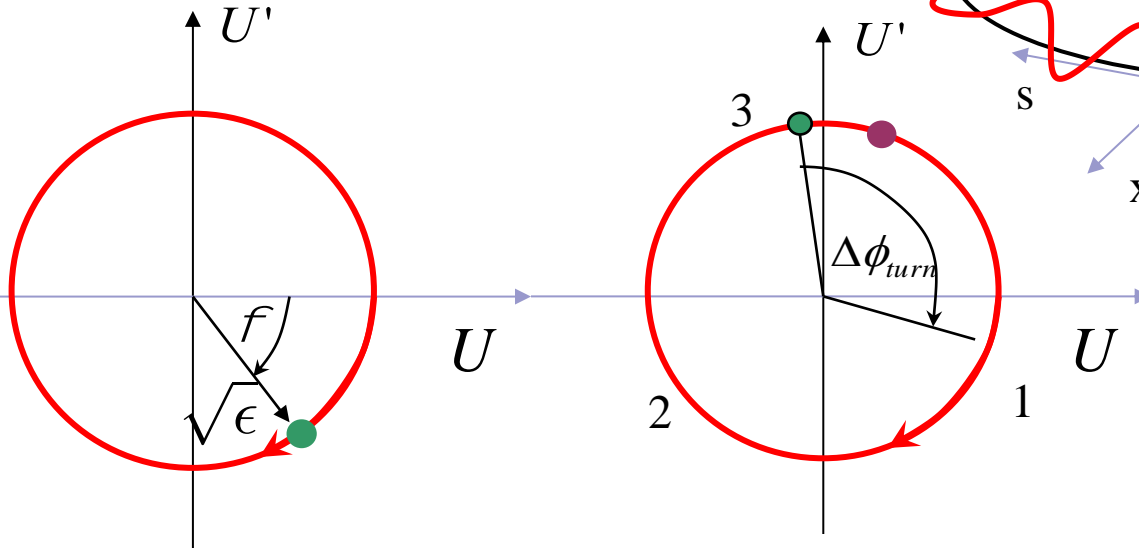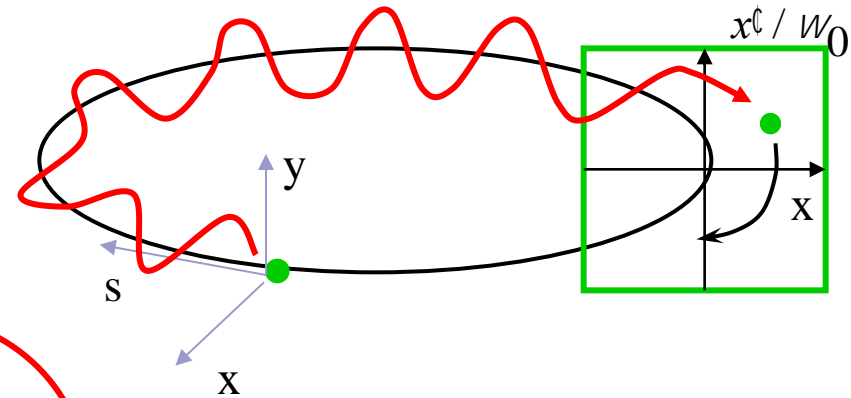


- Resonance condition corresponds to a periodic orbit or in fixed points in phase space
- For a sextupole $\delta \mathcal{U}' = \overline{b_3} \mathcal{U}^2$

- The particle does not lie on a circle!



$\Delta\phi_{turn}$

$\sqrt{\epsilon}$

$2pn_0$

$\sqrt{\epsilon} + \delta(\sqrt{\epsilon})$

$x^{\mathbb{C}} / w_0$

- In the vicinity of a third order resonance, three fixed points can be found at

$$\psi_{20} = \frac{\pi}{3} , \quad \frac{3\pi}{3} , \quad \frac{5\pi}{3} , \quad J_{20} = \left(\frac{2\delta}{3A_{3p}}\right)^2$$

- For $\dfrac{\delta}{A_{3p}} > 0$ all three points are unstable

- Close to the elliptic one at $\psi_{20} = 0$ the motion in phase space is described by circles that they get more and more distorted to end up in the "triangular" separatrix uniting the unstable fixed points



Separatrix

Unstable fixed points

$J_{20}$

unstable

$\psi_{20} = \dfrac{\pi}{3}$

stable

- The tune separation from the resonance (**stop-band width**) is $\quad \delta = \dfrac{3A_{3p}}{2} J_{20}^{1/2}$
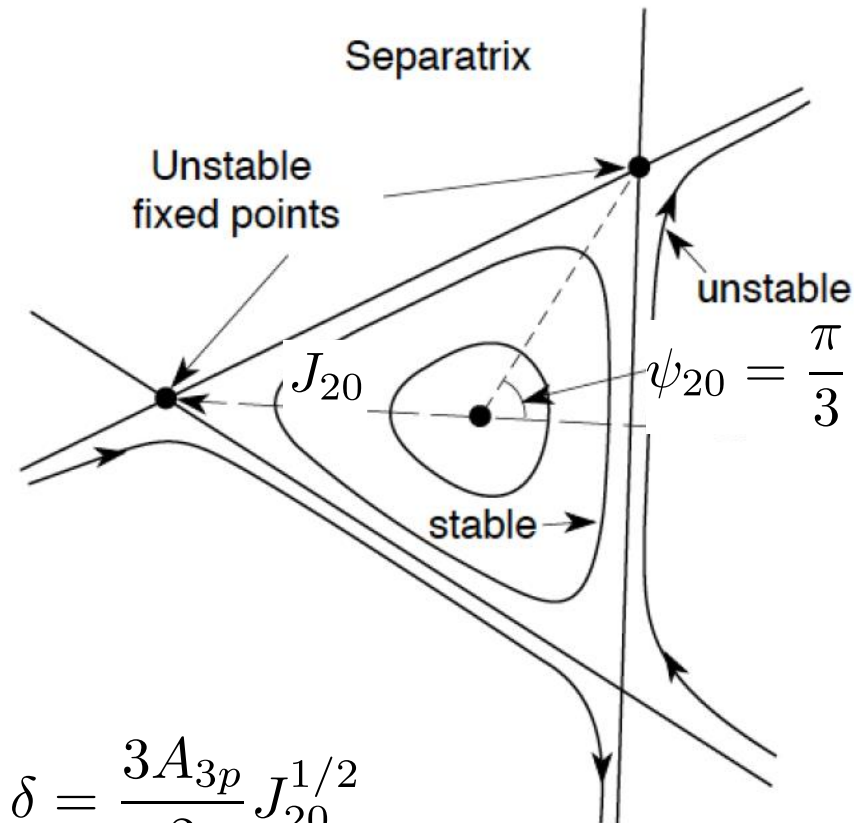
■ Regular motion near the center, with curves getting more deformed towards a rectangular shape

■ The separatrix passes through 4 unstable fixed points, but motion seems well contained

■ Four stable fixed points exist and they are surrounded by stable motion (islands of stability)
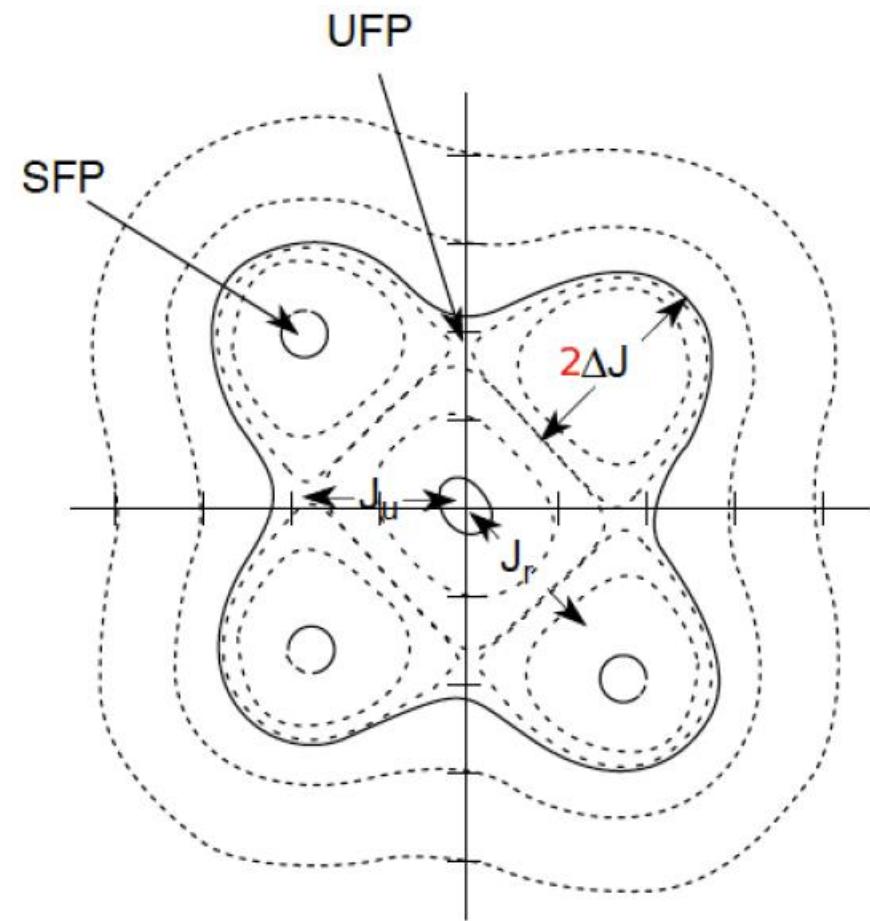
■ When perturbation becomes higher, motion around the separatrix becomes chaotic (producing tongues or splitting of the separatrix)

■ Unstable fixed points are indeed the source of chaos when a perturbation is added

# Chaotic motion
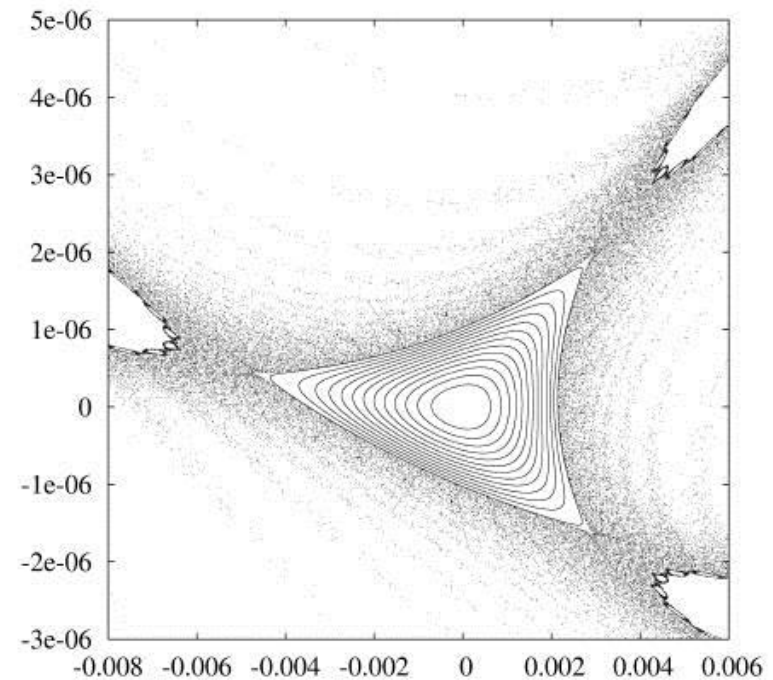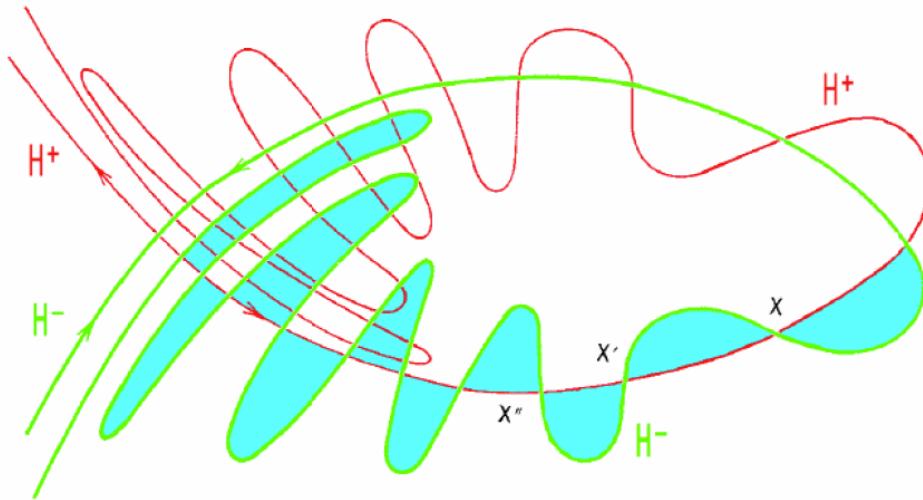
- **Poincare-Birkhoff theorem states that under perturbation of a resonance only an even number of fixed points survives (half stable and the other half unstable)**

- **Themselves get destroyed when perturbation gets higher, etc. (self-similar fixed points)**

- **Resonance islands grow and resonances can overlap allowing diffusion of particles**
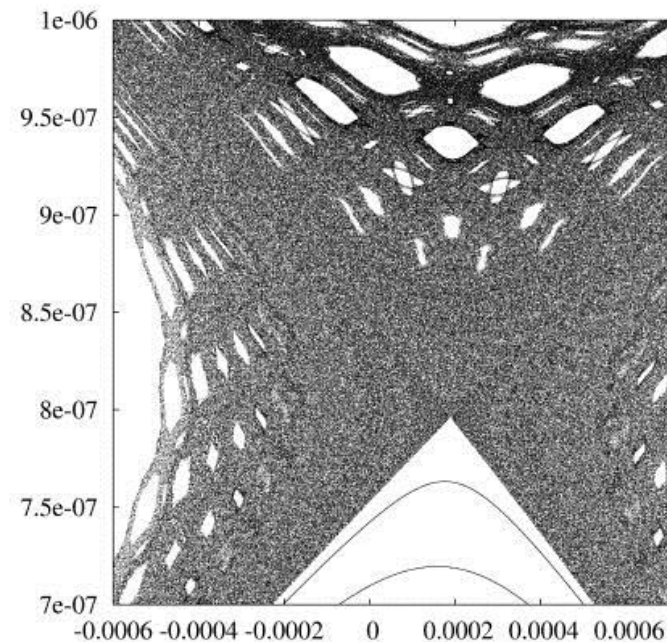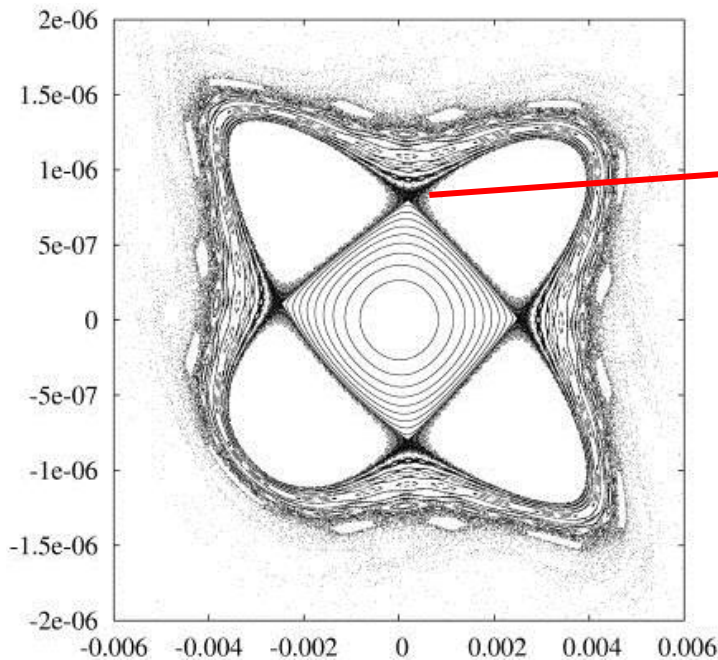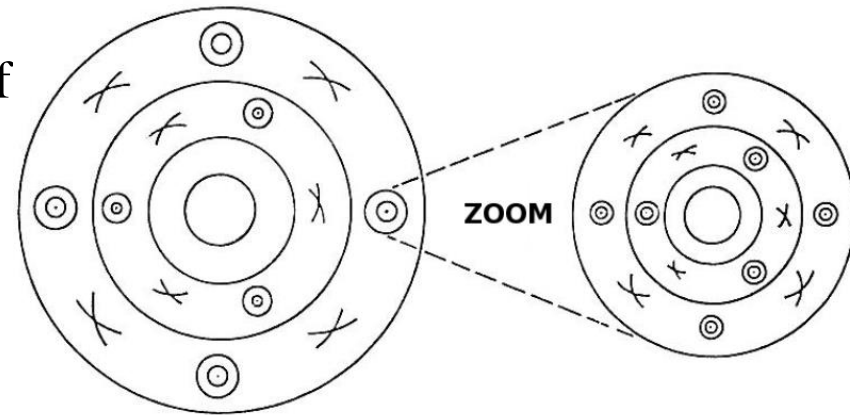
- When perturbation grows, the resonance island width grows
- **Chirikov** (1960, 1979) proposed a criterion for the overlap of two neighboring resonances and the onset of orbit diffusion
- The distance between two resonances is
$$\delta\hat{J}_{1\ n,n'} = \frac{2\left(\frac{1}{n_1+n_2} - \frac{1}{n_1'+n_2'}\right)}{\left|\frac{\partial^2 \bar{H}_0(\hat{\mathbf{J}})}{\partial \hat{J}_1^2}\bigg|_{\hat{J}_1=\hat{J}_{10}}\right|}$$
- The simple overlap criterion is
$$\Delta\hat{J}_{n\ max} + \Delta\hat{J}_{n'\ max} \geq \delta\hat{J}_{n,n'}$$
- Considering the width of chaotic layer and secondary islands, the "two thirds" rule apply $\Delta\hat{J}_{n\ max} + \Delta\hat{J}_{n'\ max} \geq \frac{2}{3}\delta\hat{J}_{n,n'}$
- The main limitation is the geometrical nature of the criterion (difficulty to be extended for > 2 degrees of freedom)
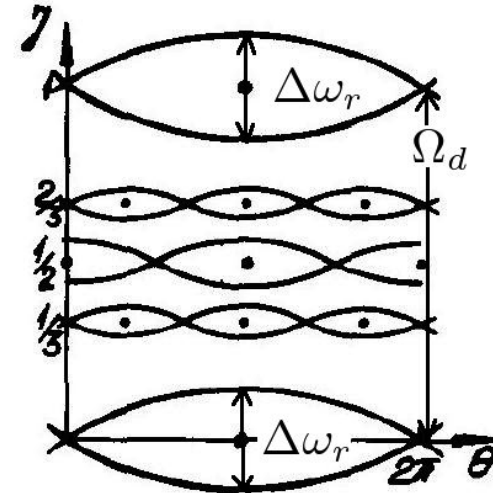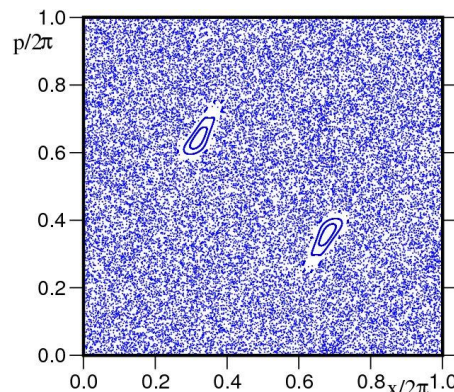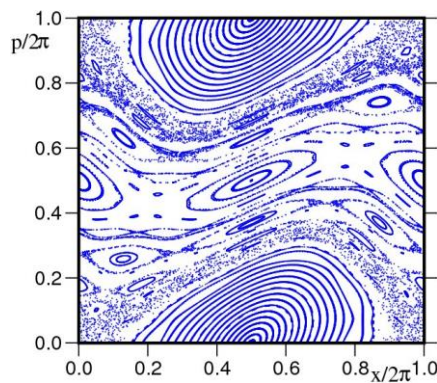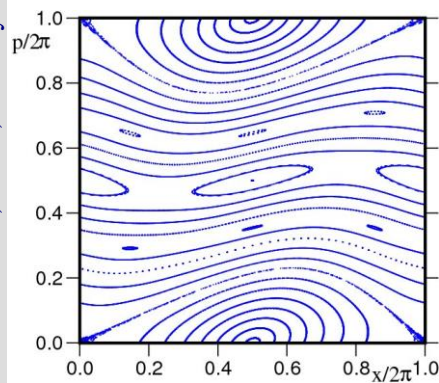
- Dynamic aperture plots often show the maximum initial values of stable trajectories in x-y coordinate space at a particular point in the lattice, for a range of energy errors.
  - ❑ The beam size (injected or equilibrium) can be shown on the same plot.
  - ❑ Generally, the goal is to allow some significant margin in the design - the measured dynamic aperture is often significantly smaller than the predicted dynamic aperture.
- This is often useful for comparison, but is not a complete characterization of the dynamic aperture: a more thorough analysis is needed for full optimization.
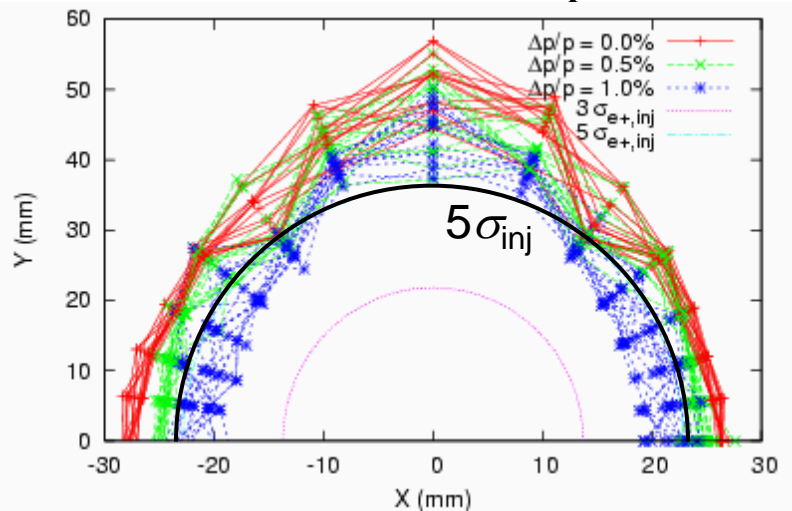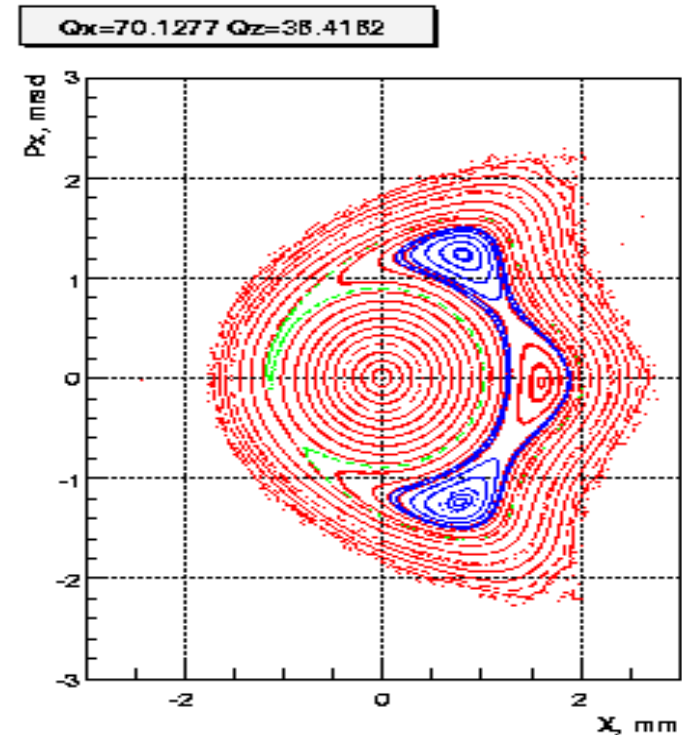
*OCS: Circular TME*
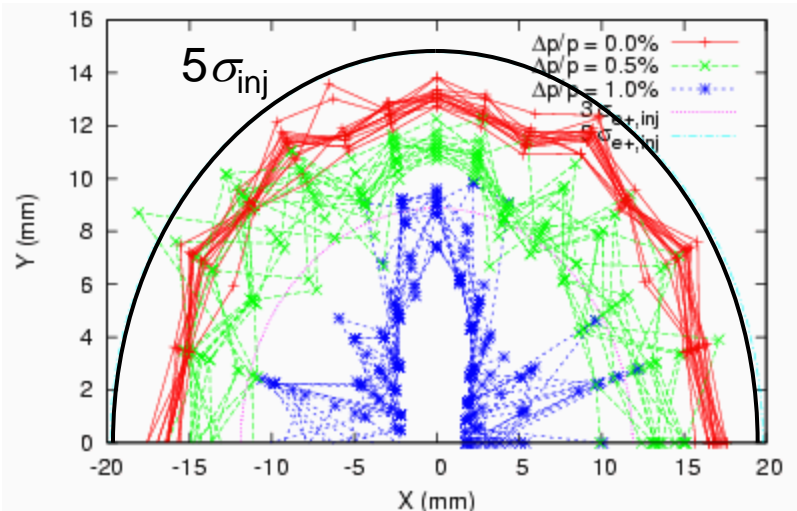
*TESLA: Dogbone TME*
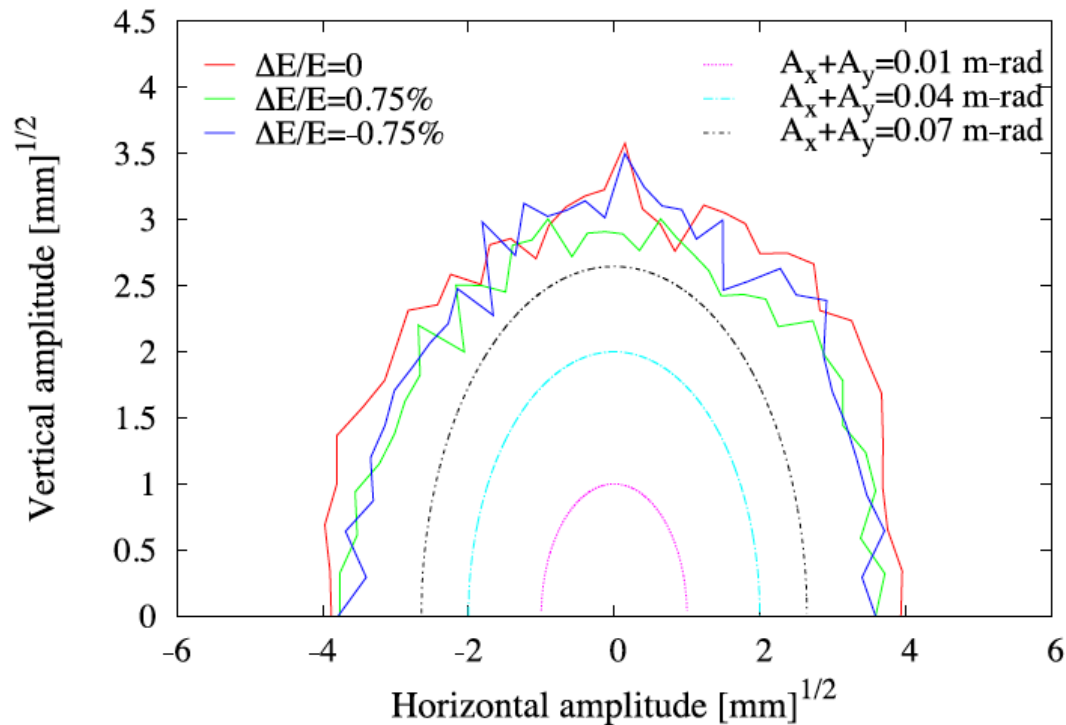
■ Dynamic aperture for lattice with specified misalignments, multipole errors, and wiggler nonlinearities

■ Specification for the phase space distribution of the injected positron bunch is an amplitude of $\mathbf{A}x + \mathbf{A}y = 0.07$m rad (normalized) and an energy spread of $\mathbf{E/E}$ 0.75%

■ DA is larger then the specified beam acceptance

Plots labeled: 0.12 ms, 0.6 ms, 1.2 ms, 1.8 ms, 2.4 ms, 3 ms, 3.6 ms, 4.2 ms, 4.8 ms
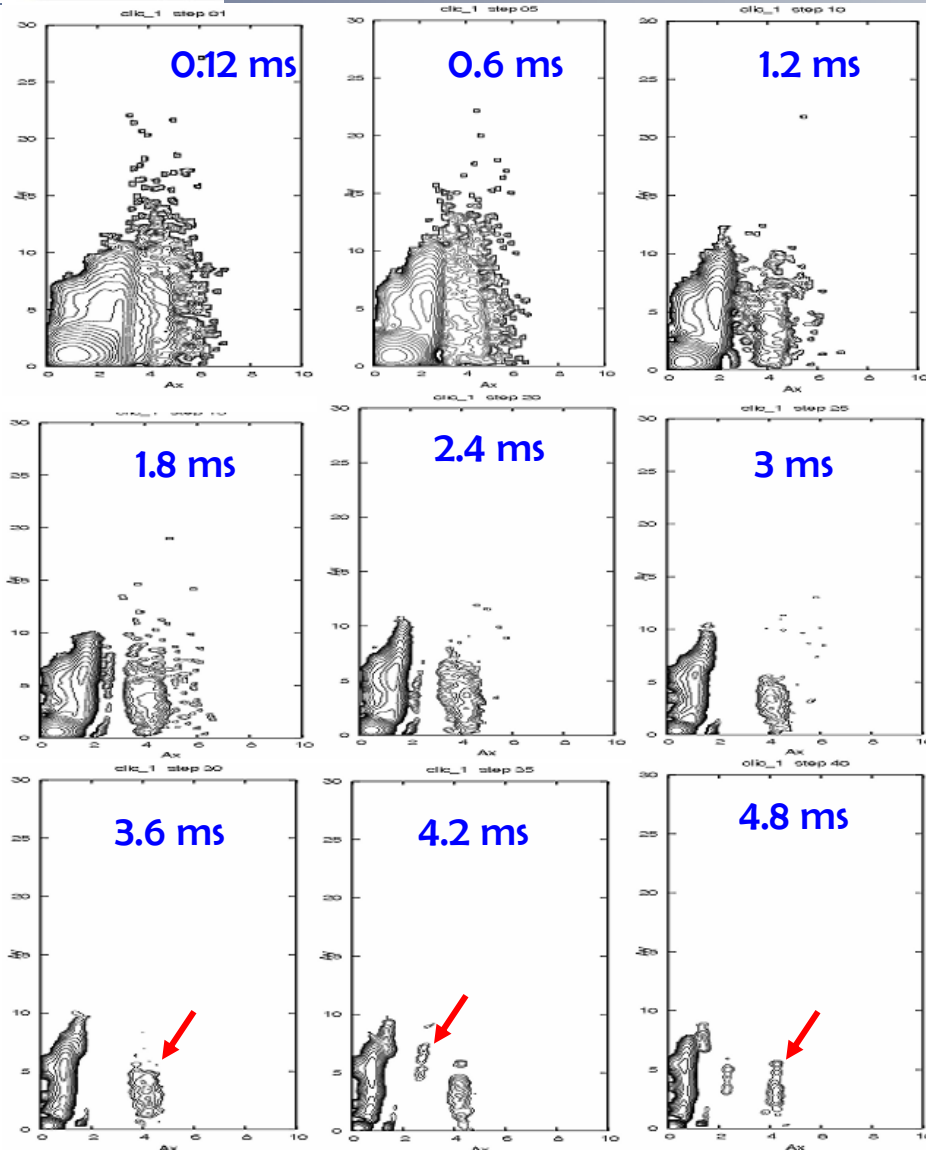
E. Levichev et al. PAC2009

Qx=70.1277 Qz=36.4182

- Including radiation damping and excitation shows that 0.7% of the particles are lost during the damping
- Certain particles seem to damp away from the beam core, on resonance islands

- Resonances and the path to chaos
  - Topology of 3$^{rd}$ and 4$^{th}$ order resonance
  - Path to chaos and resonance overlap
  - Dynamic aperture simulations
- **Frequency map analysis**
  - NAFF algorithm
  - Aspects of frequency maps
  - Frequency and diffusion maps for the LHC
  - Frequency map for lepton rings
  - Working point choice
  - Beam-beam effect
- Experiments
  - Experimental frequency maps
  - Beam loss frequency maps
  - Space-charge frequency scan

- Frequency Map Analysis (FMA) is a numerical method which springs from the studies of J. Laskar (Paris Observatory) putting in evidence the chaotic motion in the Solar Systems

- FMA was successively applied to several dynamical systems

  - Stability of Earth Obliquity and climate stabilization (Laskar, Robutel, 1993)

  - 4D maps (Laskar 1993)

  - Galactic Dynamics (Y.P and Laskar, 1996 and 1998)

  - Accelerator beam dynamics: lepton and hadron rings (Dumas, Laskar, 1993, Laskar, Robin, 1996, Y.P, 1999, Nadolski and Laskar 2001)

- When a quasi-periodic function $f(t) = q(t) + ip(t)$ in the complex domain is given numerically, it is possible to recover a quasi-periodic approximation

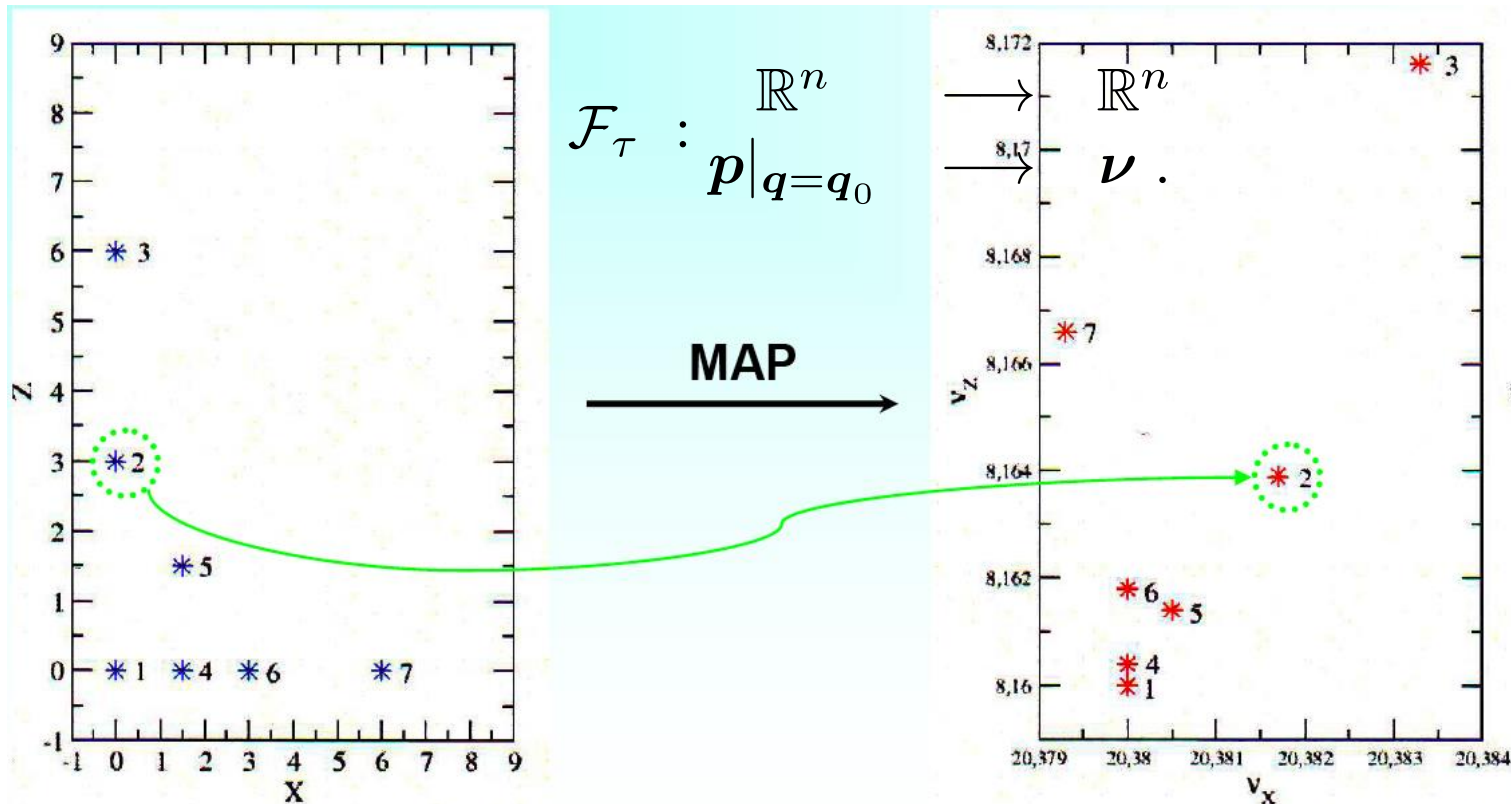$$f'(t) = \sum_{k=1}^{N} a'_k e^{i\omega'_k t}$$

  in a very precise way over a finite time span $[-T, T]$ several orders of magnitude more precisely than simple Fourier techniques

- This approximation is provided by the Numerical Analysis of Fundamental Frequencies – **NAFF** algorithm

- The frequencies $\omega'_k$ and complex amplitudes $a'_k$ are computed through an iterative scheme.

15

- In the vicinity of a resonance the system behaves like a pendulum
- Passing through the elliptic point for a fixed angle, a fixed frequency (or rotation number) is observed
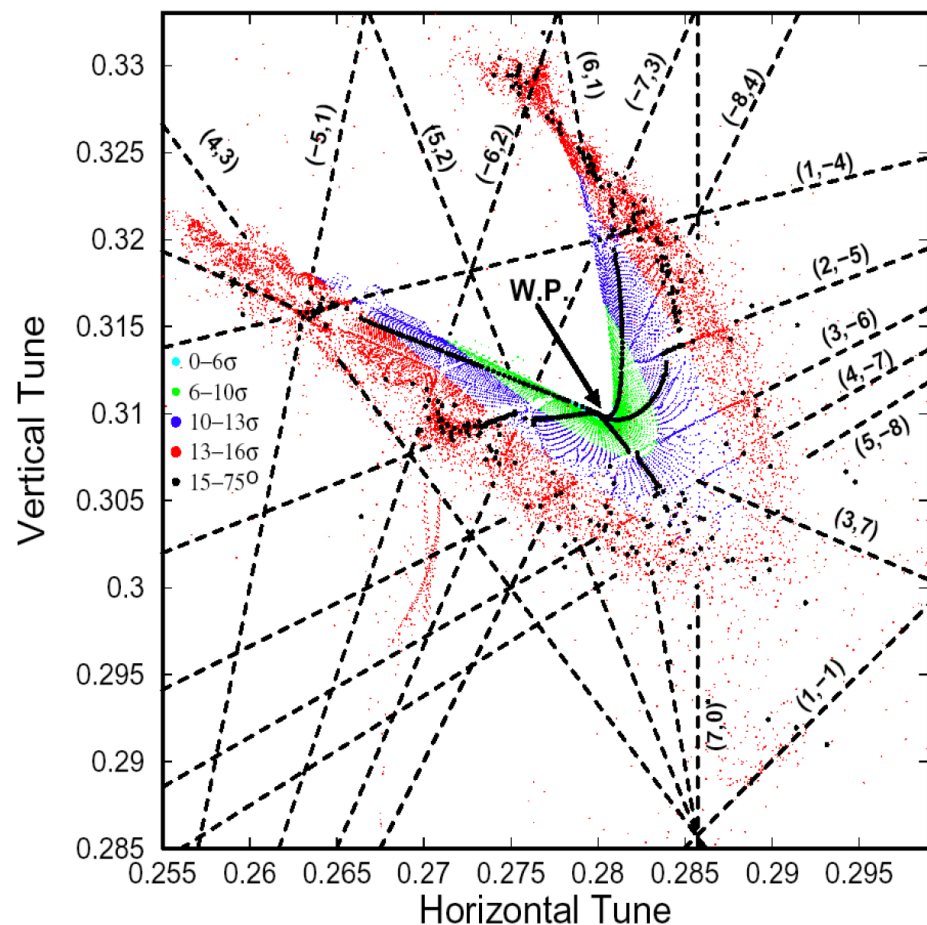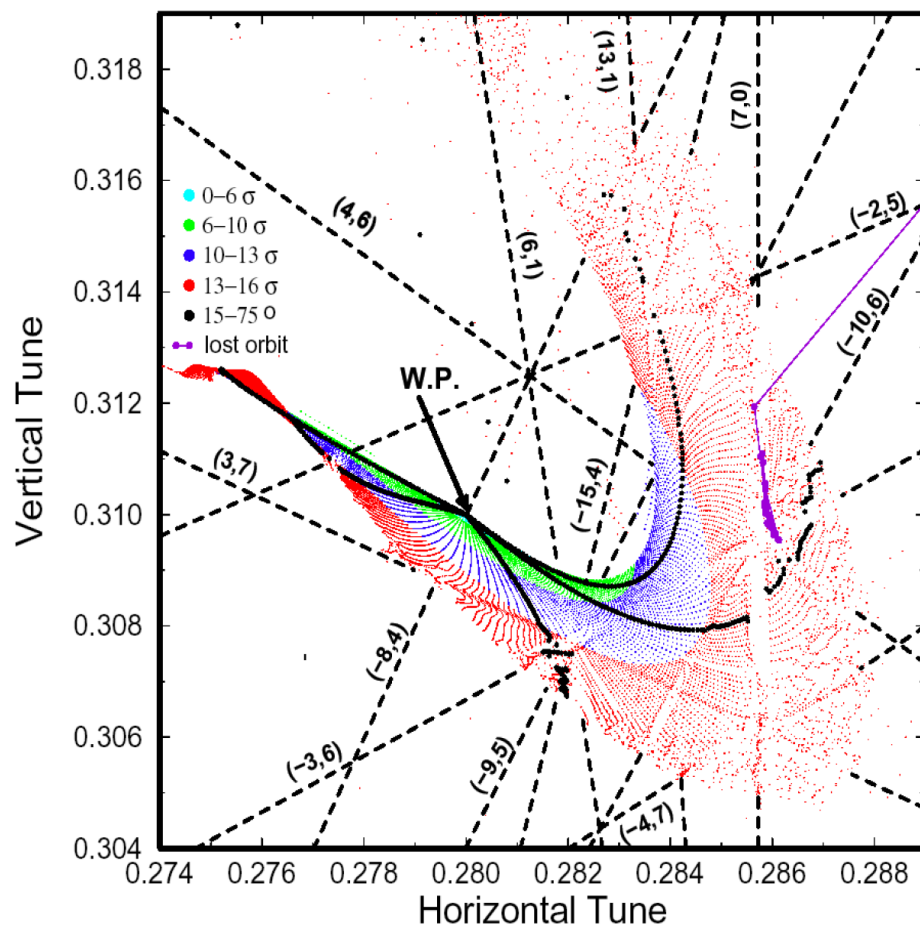- Passing through the hyperbolic point, a frequency jump is oberved
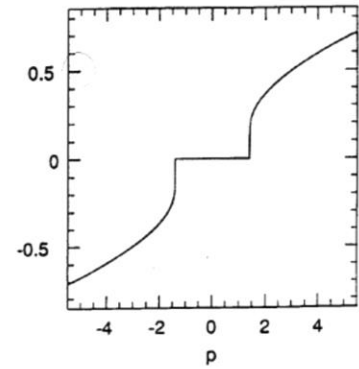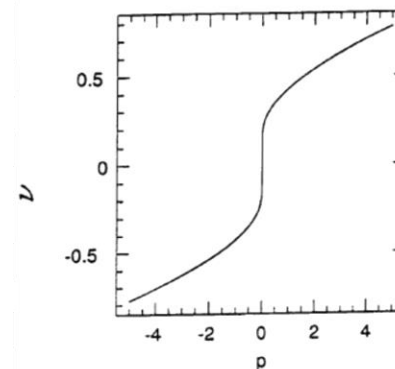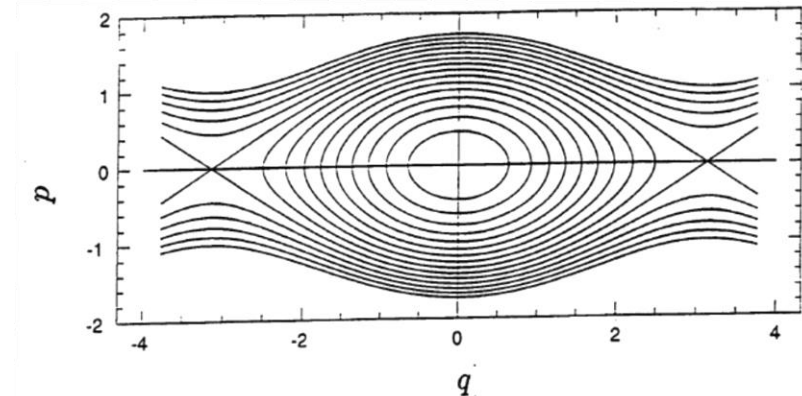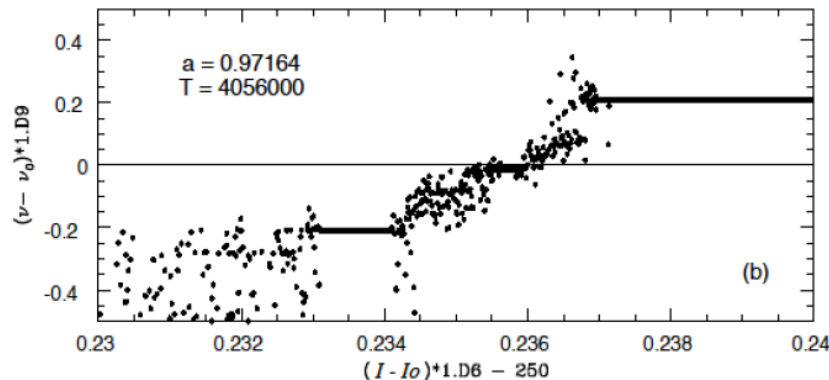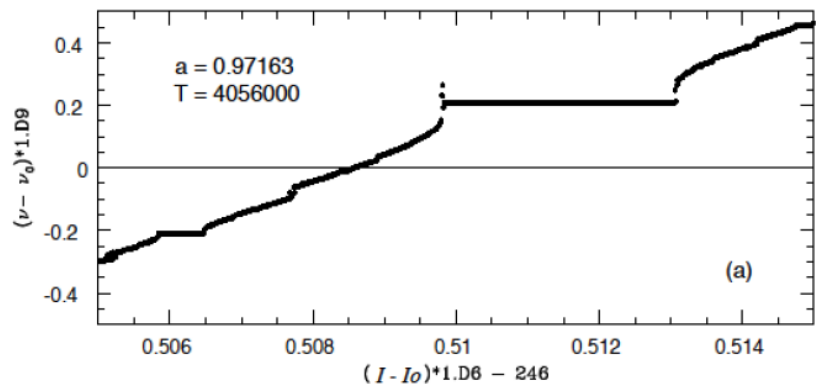
- Choose coordinates $(x_i, y_i)$ with $p_x$ and $p_y=0$

- Numerically integrate the phase trajectories through the lattice for sufficient number of turns

- Compute through NAFF $Q_x$ and $Q_y$ after sufficient number of turns

- Plot them in the tune diagram



$$\mathcal{F}_\tau : \begin{array}{c} \mathbb{R}^n \\ p|_{q=q_0} \end{array} \begin{array}{c} \longrightarrow \\ \longrightarrow \end{array} \begin{array}{c} \mathbb{R}^n \\ \nu . \end{array}$$

MAP

Frequency maps for the target error table (left) and an increased random skew octupole error in the super-conducting dipoles (right)

18

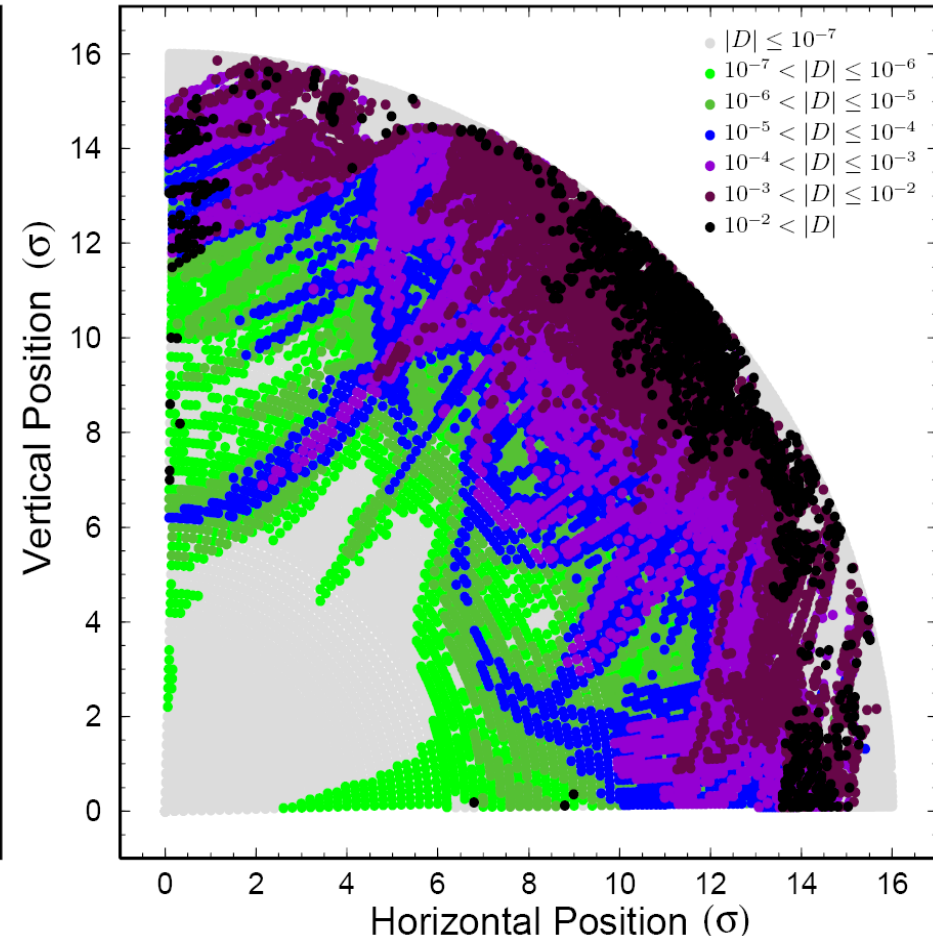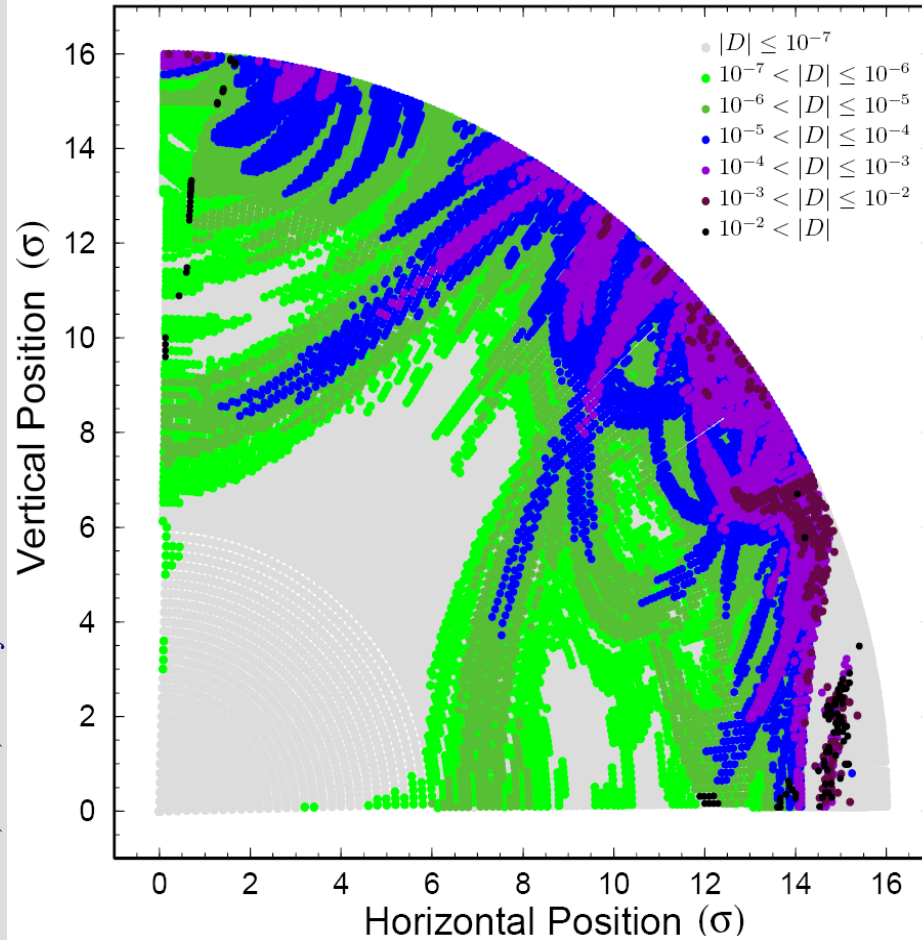■ Calculate frequencies for two equal and successive time spans and compute frequency diffusion vector:

$$D\big|_{t=\tau} = \nu\big|_{t\in(0,\tau/2]} - \nu\big|_{t\in(\tau/2,\tau]}$$

■ Plot the initial condition space color-coded with the norm of the diffusion vector

■ Compute a diffusion quality factor by averaging all diffusion coefficients normalized with the initial conditions radius

$$D_{QF} = \left\langle \frac{|D|}{(I_{x0}^2 + I_{y0}^2)^{1/2}} \right\rangle_R$$

Diffusion maps for the target error table (left) and an increased random skew octupole error in the super-conducting dipoles (right)
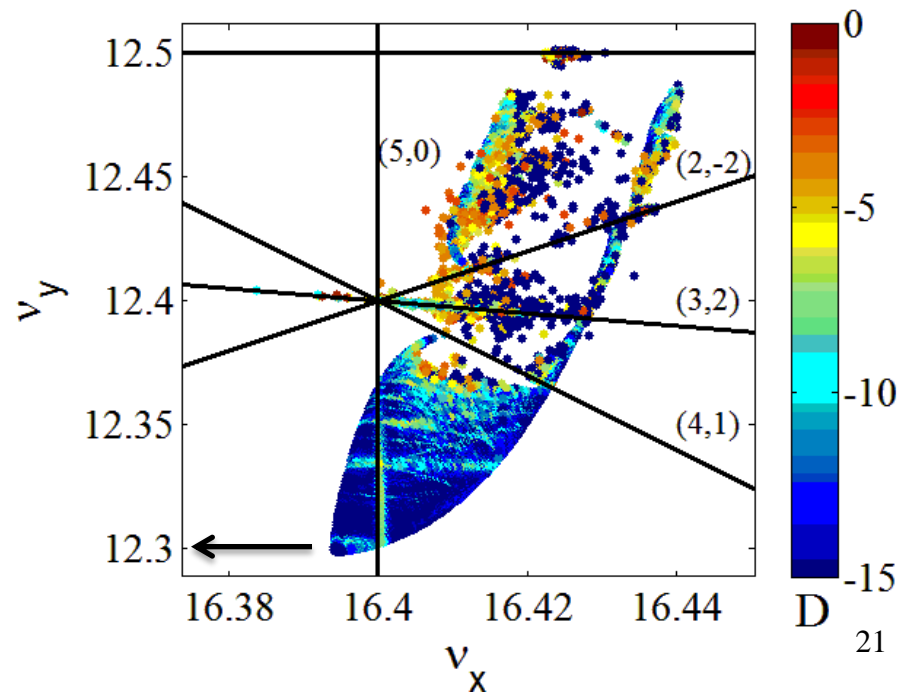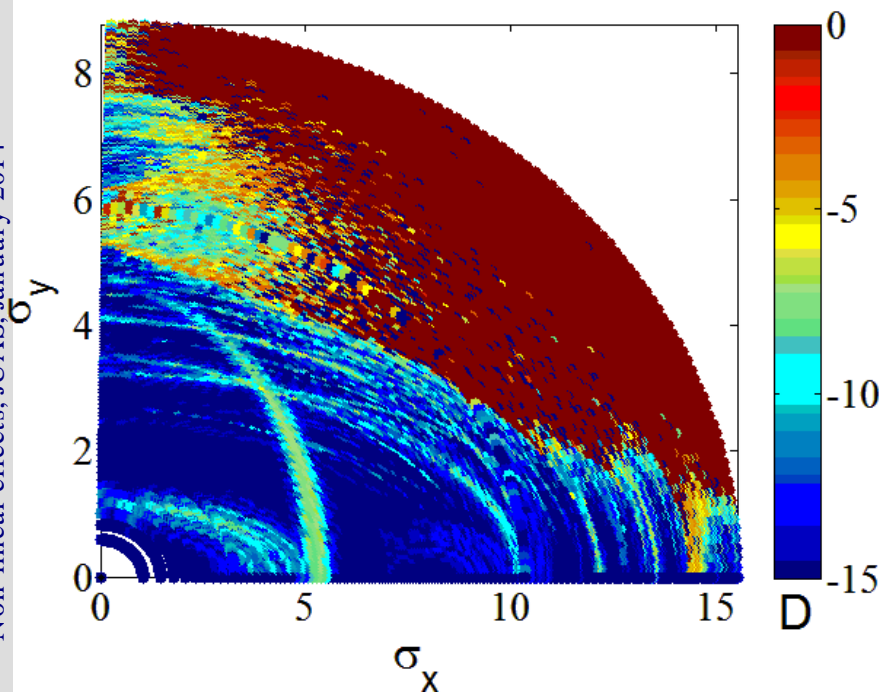
- Non linear optimization based on phase advance scan for minimization of resonance driving terms and tune-shift with amplitude
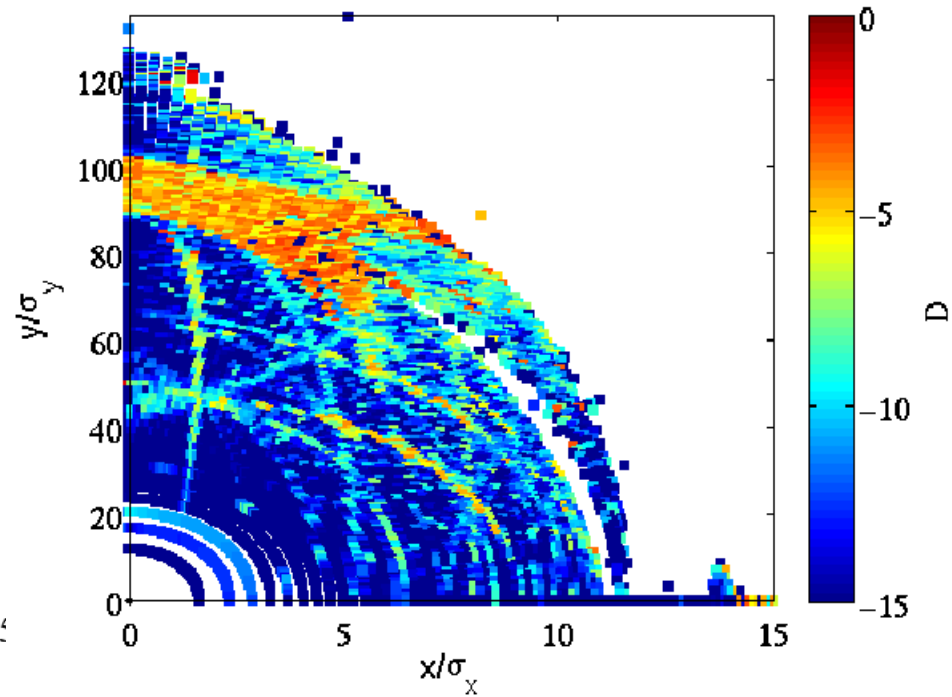
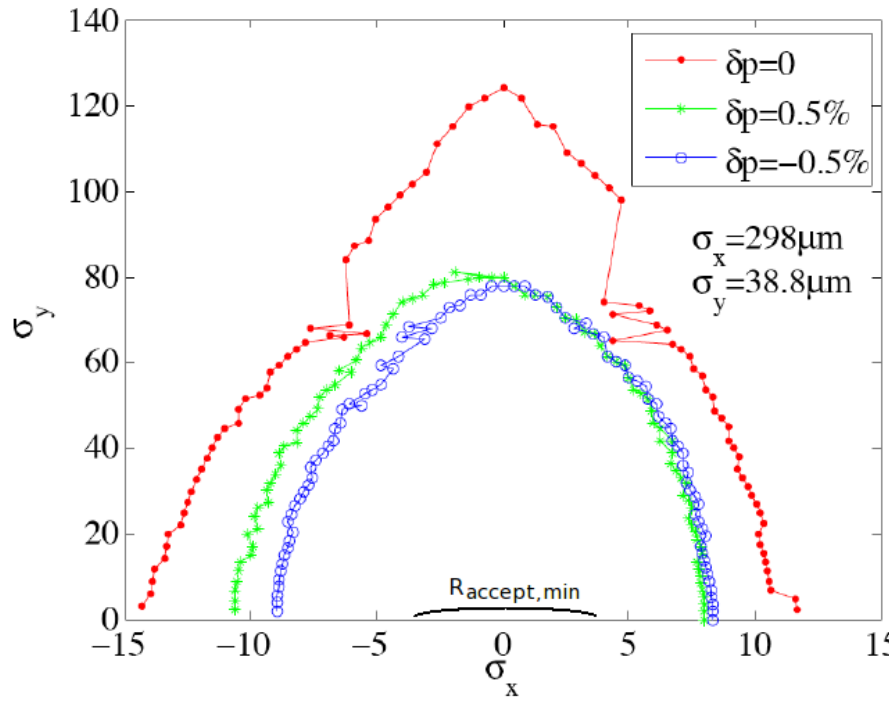$$\left| \sum_{p=0}^{N_c-1} e^{ip(n_x m_{x,c} + n_y m_{y,c})} \right| = \sqrt{\frac{1 - \cos\left[ N_c(n_x m_{x,c} + n_y m_{y,c}) \right]}{1 - \cos(n_x m_{x,c} + n_y m_{y,c})}} = 0$$

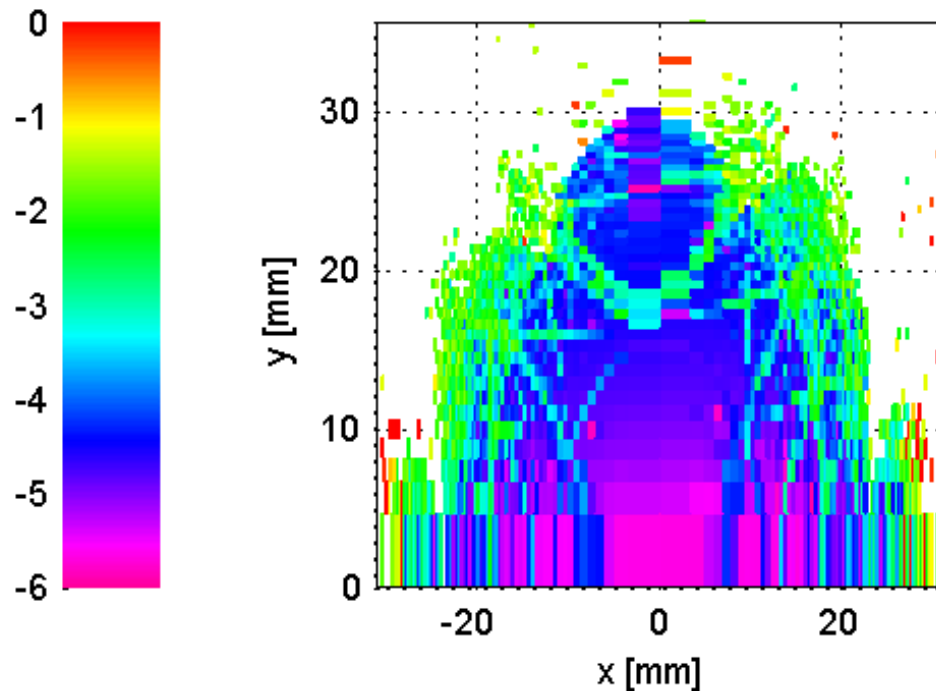$$N_c(n_x m_{x,c} + n_y m_{y,c}) = 2k\pi$$

$$n_x m_{x,c} + n_y m_{y,c} \neq 2k'\pi$$

- **Dynamic aperture and diffusion map**
- **Very comfortable DA especially in the vertical plane**
  - Vertical beam size very small, to be reviewed especially for removing electron PDR
- **Need to include non-linear fields of magnets and wigglers**
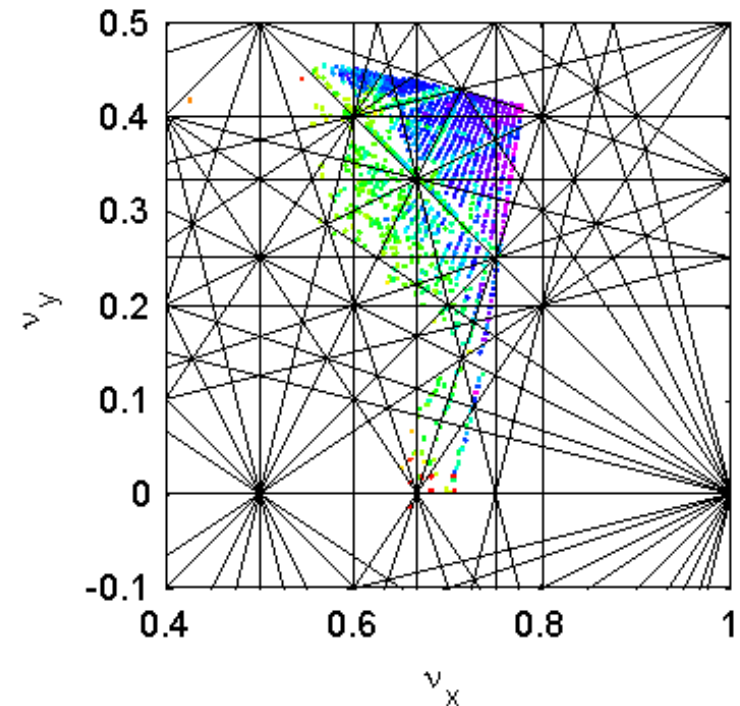
- Frequency maps enabled the comparison and steering of different lattice designs with respect to non-linear dynamics
  - ❑ Working point optimisation, on and off-momentum dynamics, effect of multi-pole errors in wigglers

■ All dynamics represented in these two plots

■ Regular motion represented by blue colors (close to zero amplitude particles or working point)
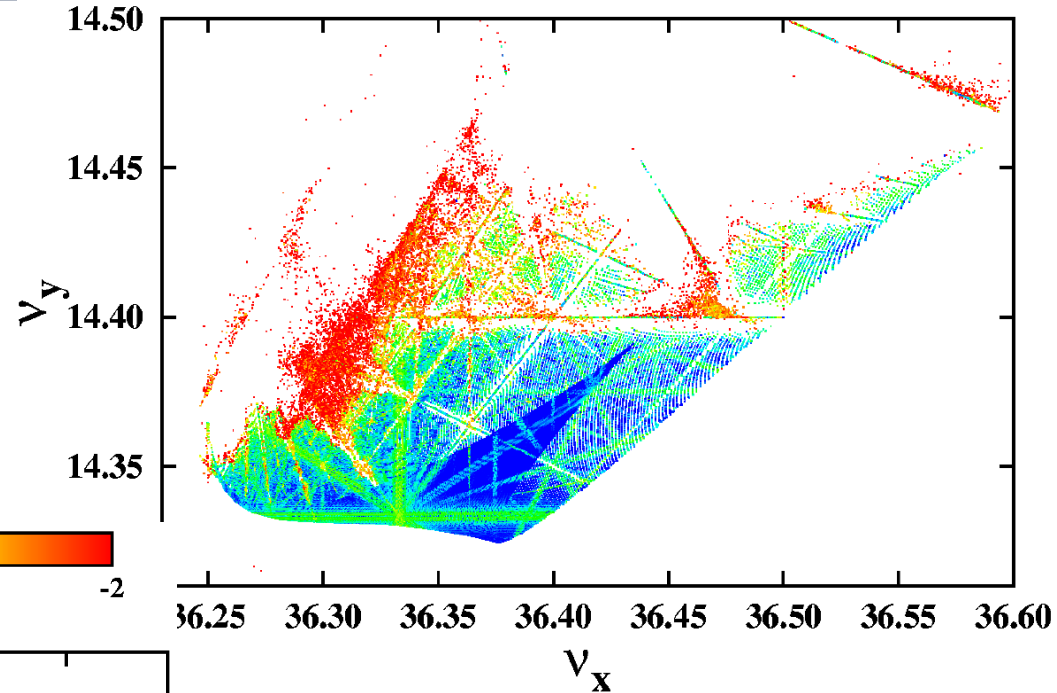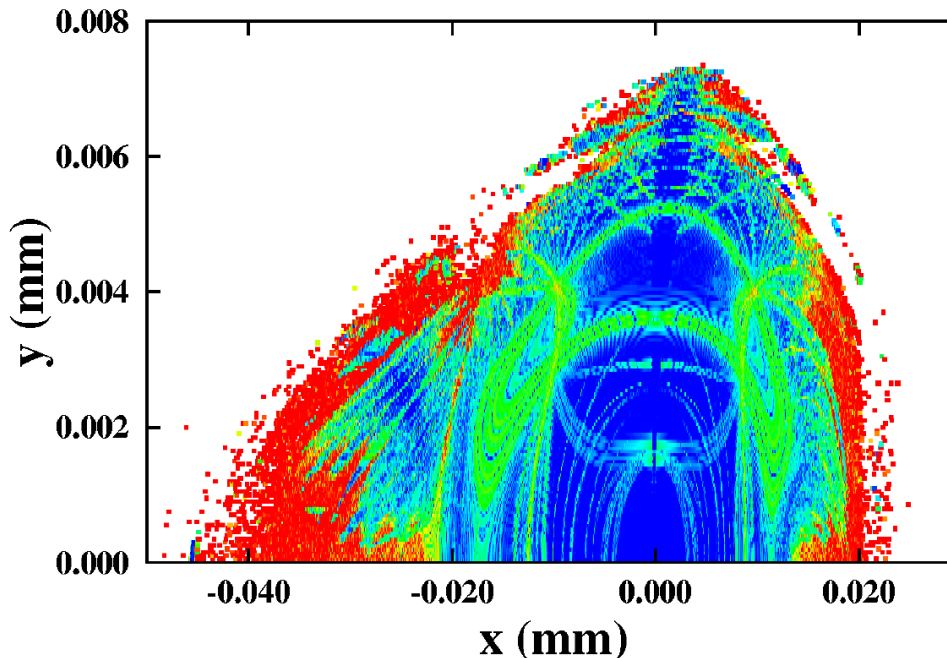


■ Resonances appear as distorted lines in frequency space (or curves in initial condition space
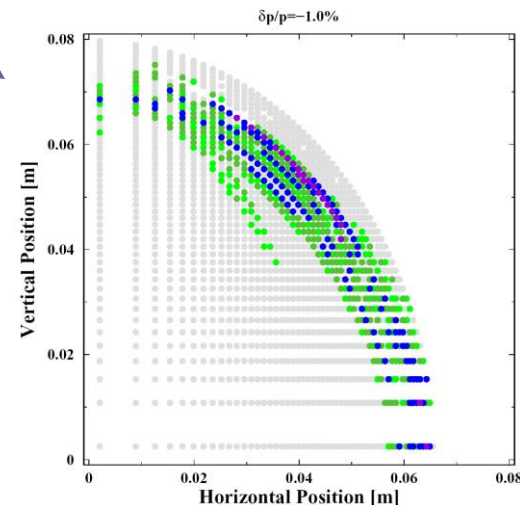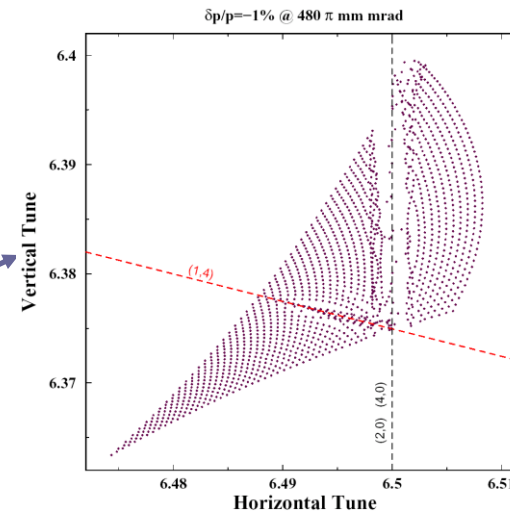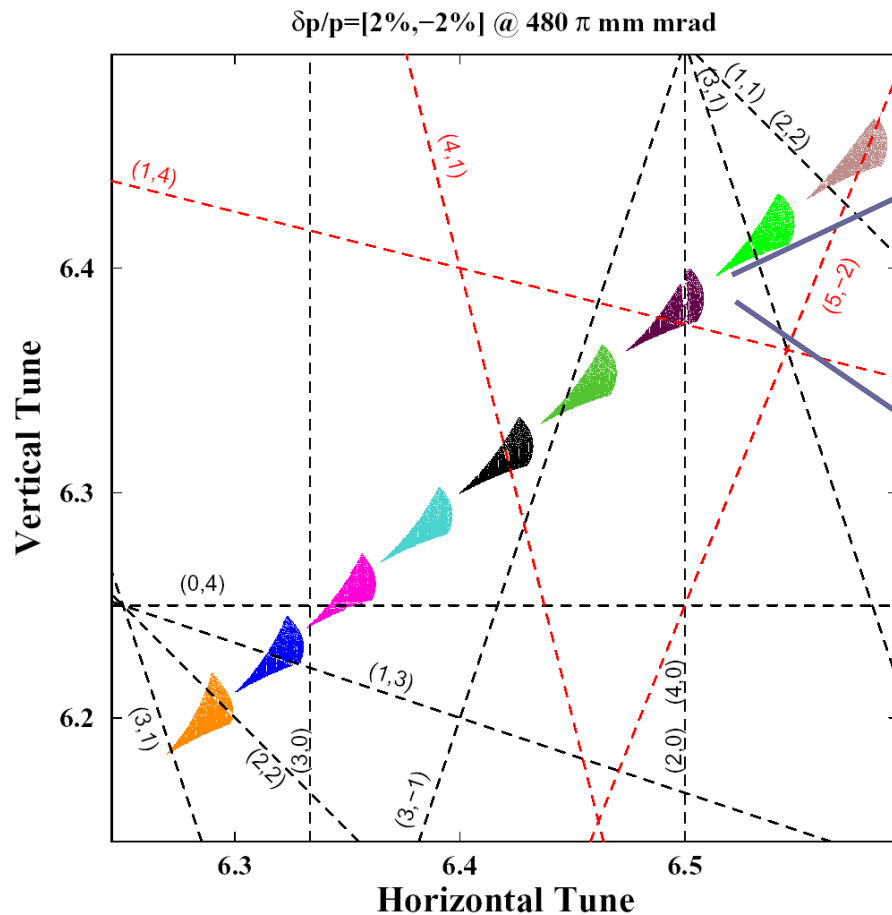
■ Chaotic motion is represented by red scattered particles and defines dynamic aperture of the machine

- Integrate a large number of particles
- Calculate the tune with refined Fourier analysis

$$\mathcal{F}_\tau \ : \ \begin{array}{ccc} \mathbb{R}^2 & \longrightarrow & \mathbb{R}^2 \\ (I_x, I_y)|_{p_x, p_y = 0}, & \longrightarrow & (\nu_x, \nu_y) \end{array}$$

- Plot points to tune space

**SNS Working Point $(Q_x, Q_y) = (6.4, 6.3)$**



$\delta p/p = [2\%, -2\%] @ 480 \pi$ mm mrad



$\delta p/p = -1\% @ 480 \pi$ mm mrad



$\delta p/p = -1.0\%$

- $|D| \leq 10^{-7}$
- $10^{-7} < |D| \leq 10^{-6}$
- $10^{-6} < |D| \leq 10^{-5}$
- $10^{-5} < |D| \leq 10^{-4}$
- $10^{-4} < |D| \leq 10^{-3}$
- $10^{-3} < |D| \leq 10^{-2}$
- $10^{-2} < |D|$

$\delta p/p=0$ @ $480\,\pi$ mm mrad

$\delta p/p=0$
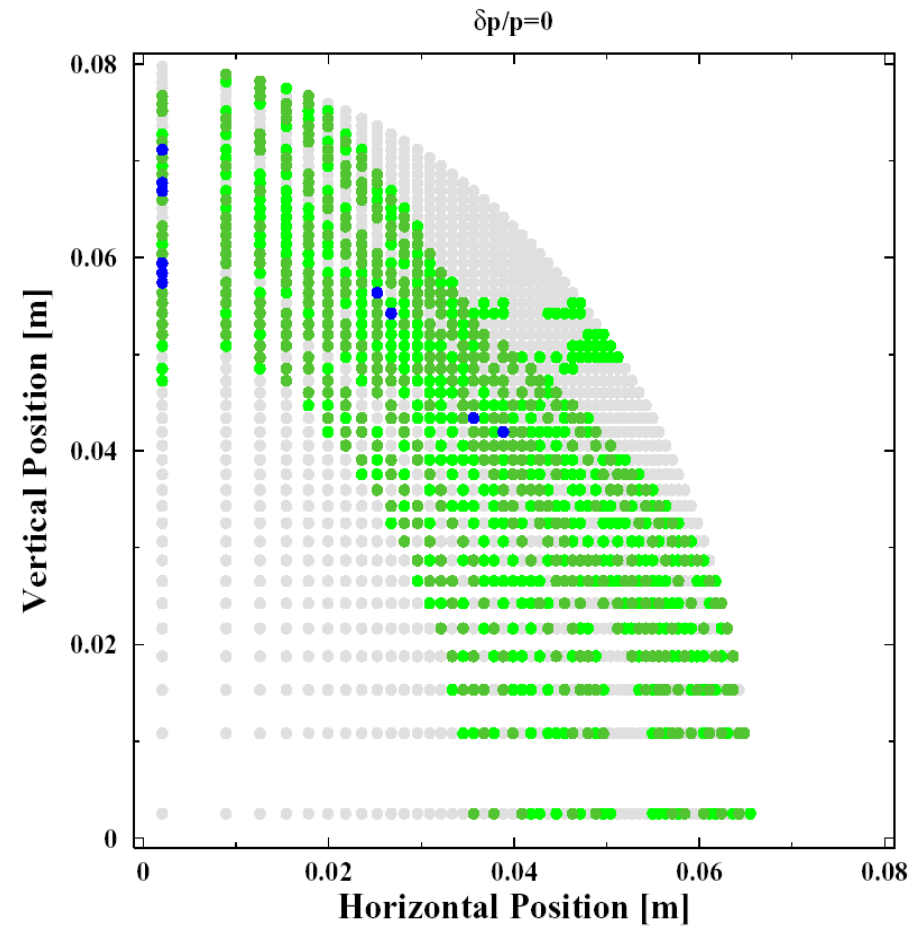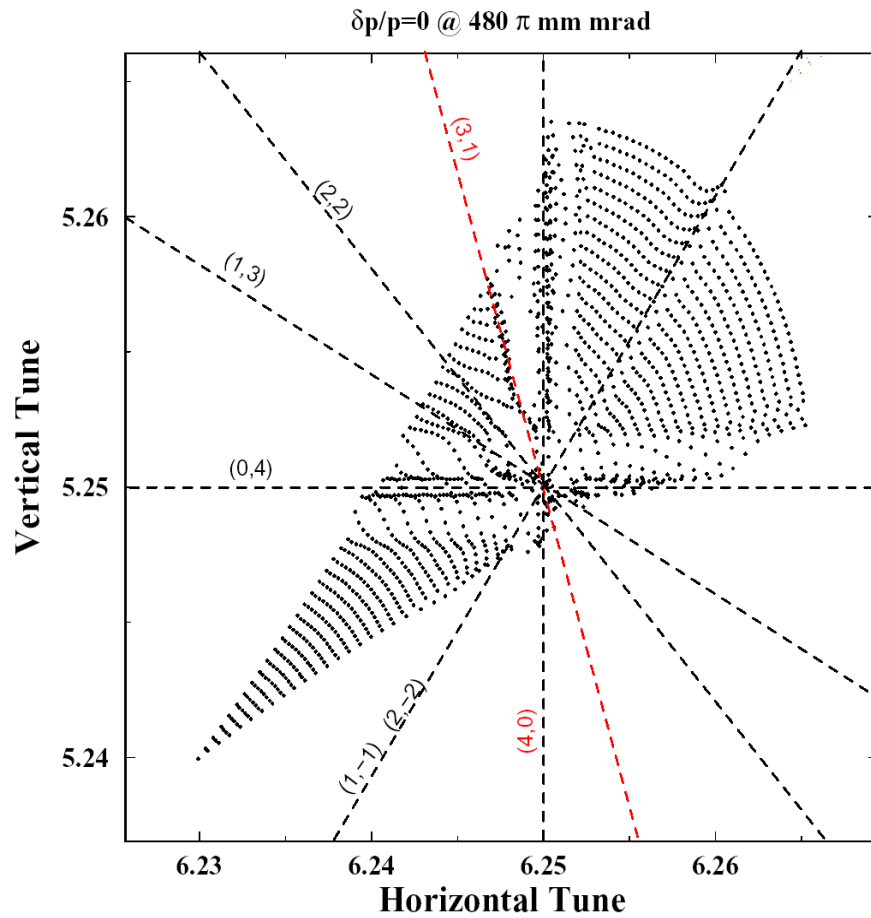
Tune Diffusion quality factor

$$D_{QF} = \Big\langle \frac{|\boldsymbol{D}|}{(I_{x0}^2 + I_{y0}^2)^{1/2}} \Big\rangle_R$$

**Working point comparison (no sextupoles)**
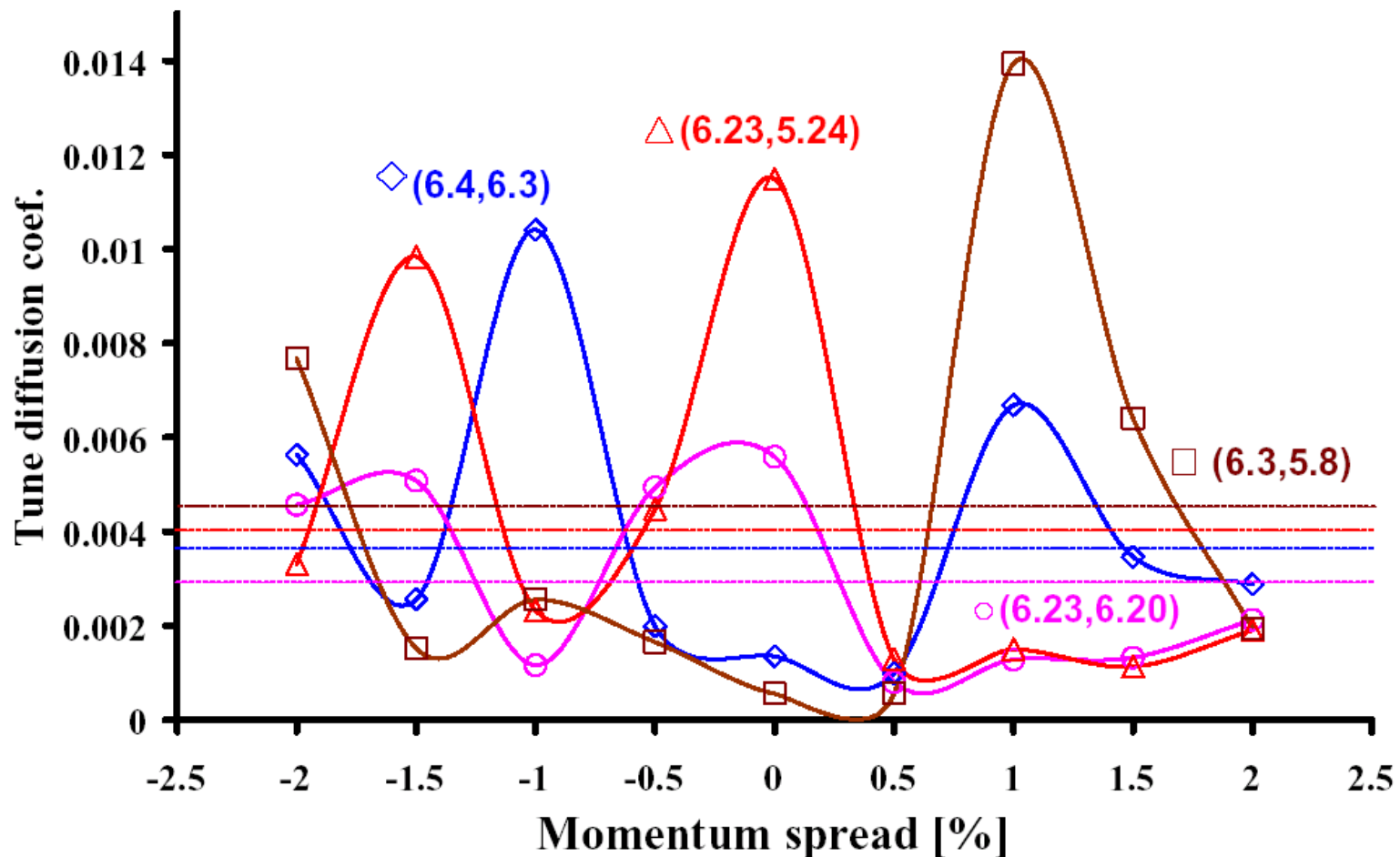
- Figure of merit for choosing best working point is sum of diffusion rates with a constant added for every lost particle

- Each point is produced after tracking 100 particles

- Nominal working point had to be moved towards "blue" area

S. Liuzzo et al., IPAC 2012



$$e^D = \sqrt{\frac{(\nu_{x,1} - \nu_{x,2})^2 + (\nu_{y,1} - \nu_{y,2})^2}{N/2}}$$

$$WPS = 0.1 N_{lost} + \sum e^D$$

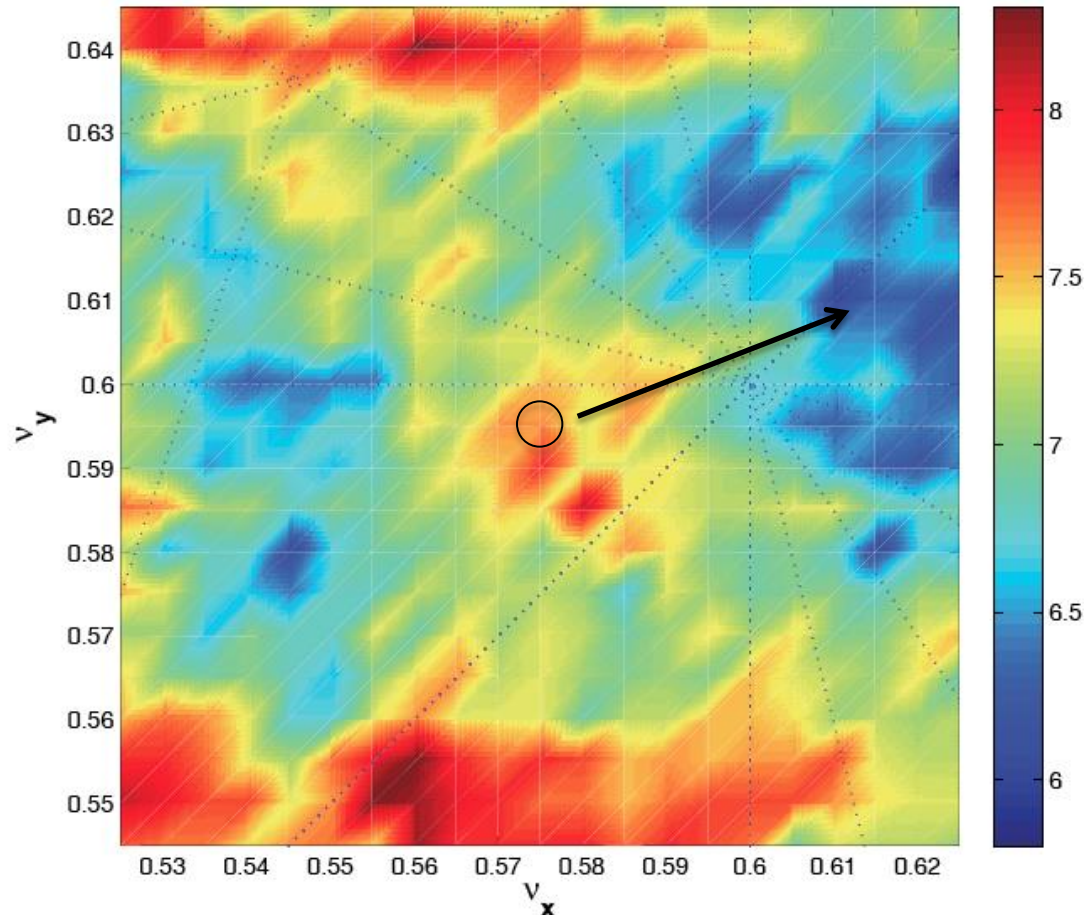| Variable | Symbol | Value |
|---|---|---|
| Beam energy | $E$ | 7 TeV |
| Particle species | $\cdots$ | protons |
| Full crossing angle | $\theta_c$ | 300 $\mu$rad |
| rms beam divergence | $\sigma_x'$ | 31.7 $\mu$rad |
| rms beam size | $\sigma_x$ | 15.9 $\mu$m |
| Normalized transv. rms emittance | $\gamma\varepsilon$ | 3.75 $\mu$m |
| IP beta function | $\beta^*$ | 0.5 m |
| Bunch charge | $N_b$ | $(1\times10^{11}$–$2\times10^{12})$ |
| Betatron tune | $Q_0$ | 0.31 |

■ Long range beam-beam interaction represented by a 4D kick-map



$$\Delta x = -\, n_{par}\; \frac{2r_p N_b}{\gamma}\; \left[\; \frac{x'+\theta_c}{\theta_t^2}\; \left(1 - e^{-\frac{\theta_t^2}{2\theta_{x,y}^2}}\right)\right.$$

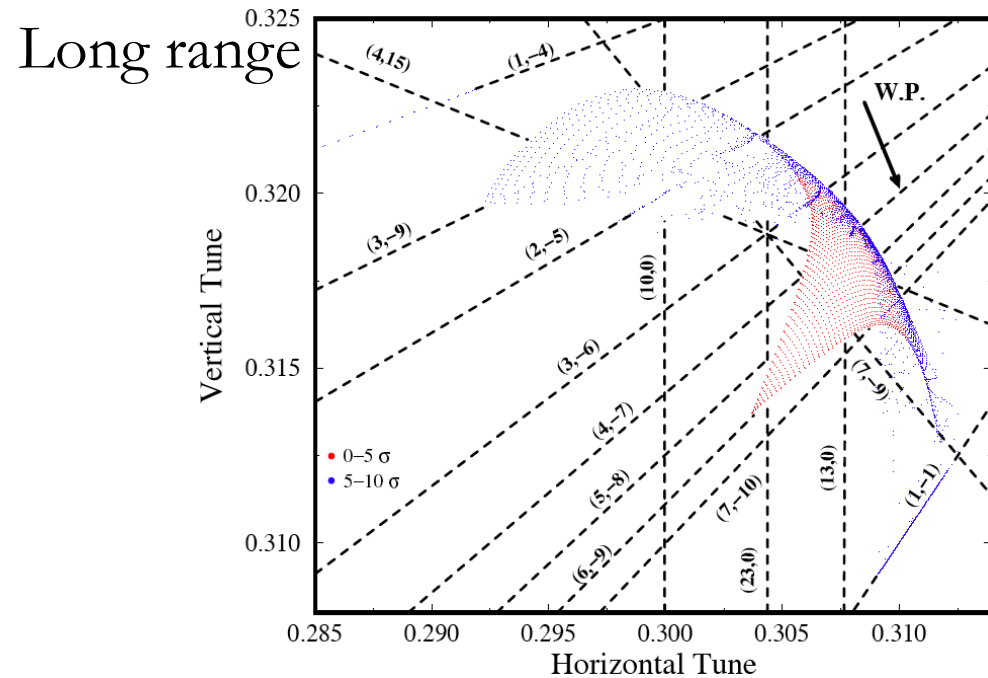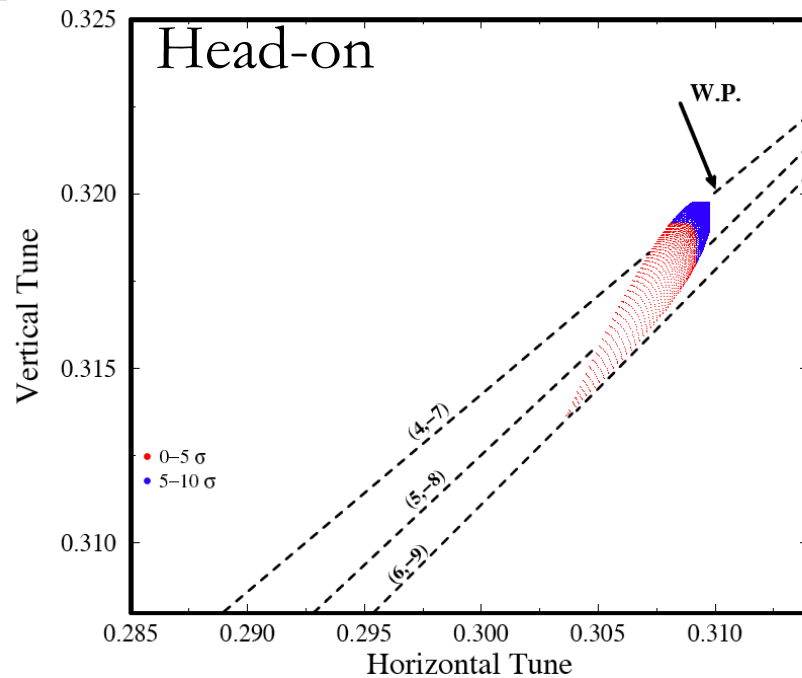$$\left. -\, \frac{1}{\theta_c}\left(1 - e^{-\frac{\theta_c^2}{2\theta_{x,y}^2}}\right)\;\right]$$

$$\Delta y = -\, n_{par}\; \frac{2r_p N_b}{\gamma}\; \frac{y'}{\theta_t^2}\; \left(1 - e^{-\frac{\theta_t^2}{2\theta_{x,y}^2}}\right)$$

with $\qquad \theta_t \equiv \left((x'+\theta_c)^2 + y'^2\right)^{1/2}$
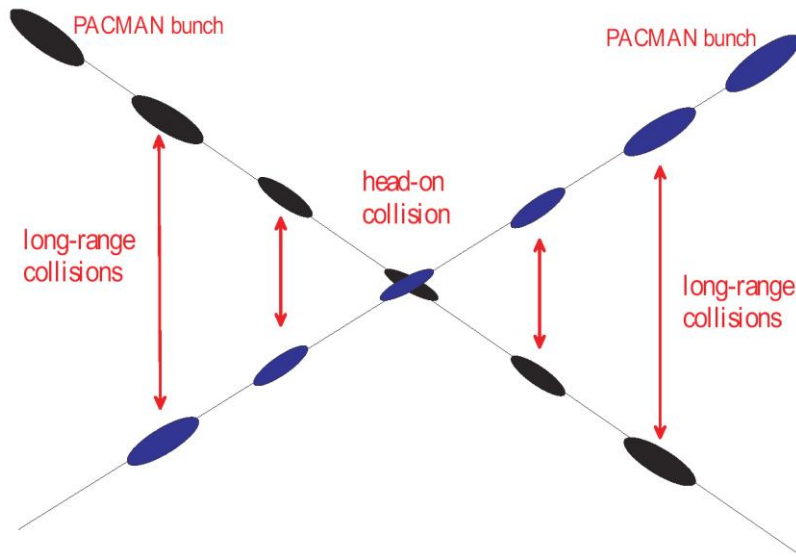
YP and F. Zimmermann, PRSTAB 1999, 2002



- Proved dominant effect of long range beam-beam effect
- Dynamic Aperture (around 6σ) located at the folding of the map (indefinite torsion)
- Dynamics dominated by the 1/r part of the force, reproduced by electrical wire, which was proposed for correcting the effect
- Experimental verification in SPS and installation to the LHC IPs

- Resonances and the path to chaos
  - Topology of 3$^{rd}$ and 4$^{th}$ order resonance
  - Path to chaos and resonance overlap
  - Dynamic aperture simulations
- Frequency map analysis
  - NAFF algorithm
  - Aspects of frequency maps
  - Frequency and diffusion maps for the LHC
  - Frequency map for lepton rings
  - Working point choice
  - Beam-beam effect
- **Experiments**
  - Experimental frequency maps
  - Beam loss frequency maps
  - Space-charge frequency scan

D. Robin, C. Steier, J. Laskar, and L. Nadolski, PRL 2000

- Frequency analysis of turn-by-turn data of beam oscillations produced by a fast kicker magnet and recorded on a Beam Position Monitors

- Reproduction of the non-linear model of the Advanced Light Source storage ring and working point optimization for increasing beam lifetime

ALS lattice, measured frequency map (relative beamloss)



ALS lattice, measured frequency map (relative beamloss)
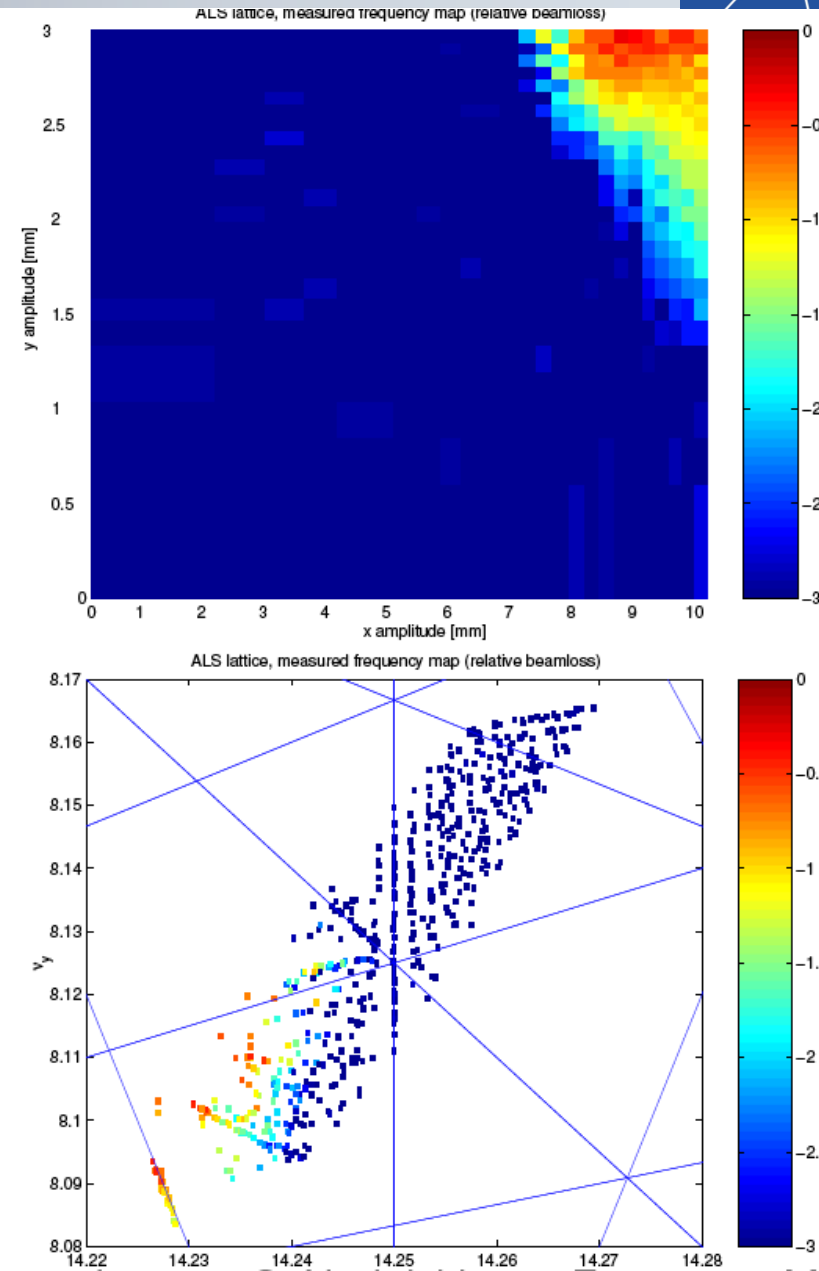
- Study the resonance behavior around different working points in SPS
- Strength of individual resonance lines can be identified from the beam loss rate, i.e. the derivative of the beam intensity at the moment of crossing the resonance
- Vertical tune is scanned from about 0.45 down to 0.05 during a period of 3s along the flat bottom
- Low intensity 4-5e10 p/b single bunches with small emittance injected
- Horizontal tune is constant during the same period
- Tunes are continuously monitored using tune monitor (tune post-processed with NAFF) and the beam intensity is recorded with a beam current transformer
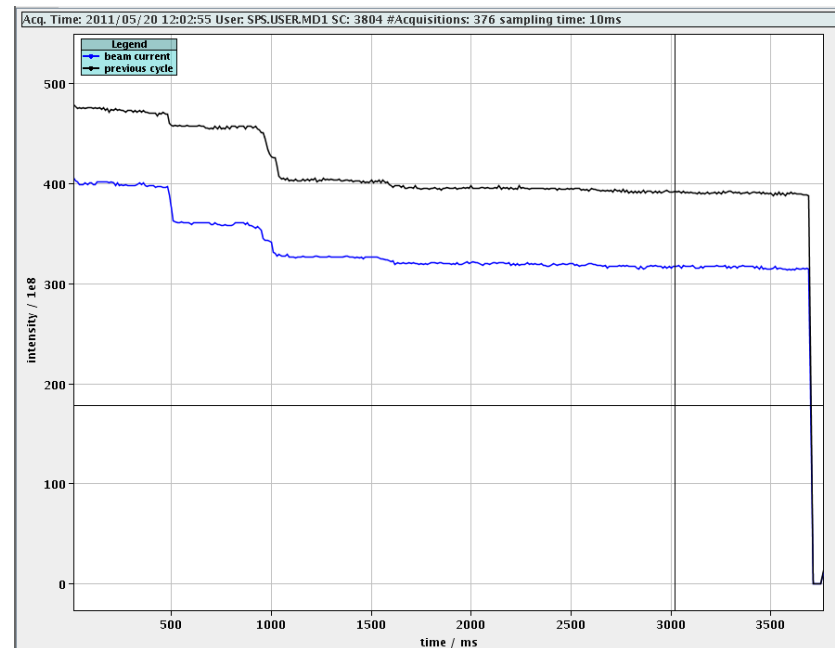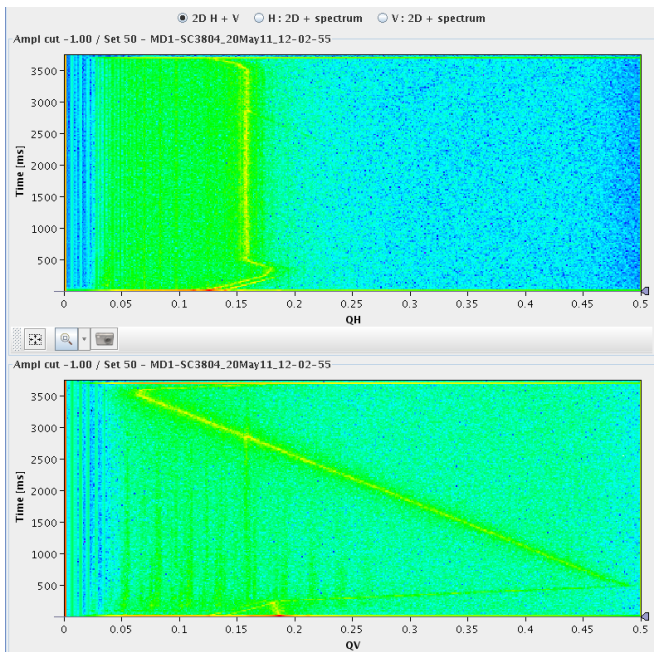
❑ **Resonances in low $\gamma_t$ optics**

- ❑ Normal sextupole Qx+2Qy is the strongest

- ❑ Skew sextupole 2Qx+Qy quite strong

- ❑ Normal sextupole Qx-2Qy, skew sextupole at 3Qy and 2Qx+2Qy fourth order visible
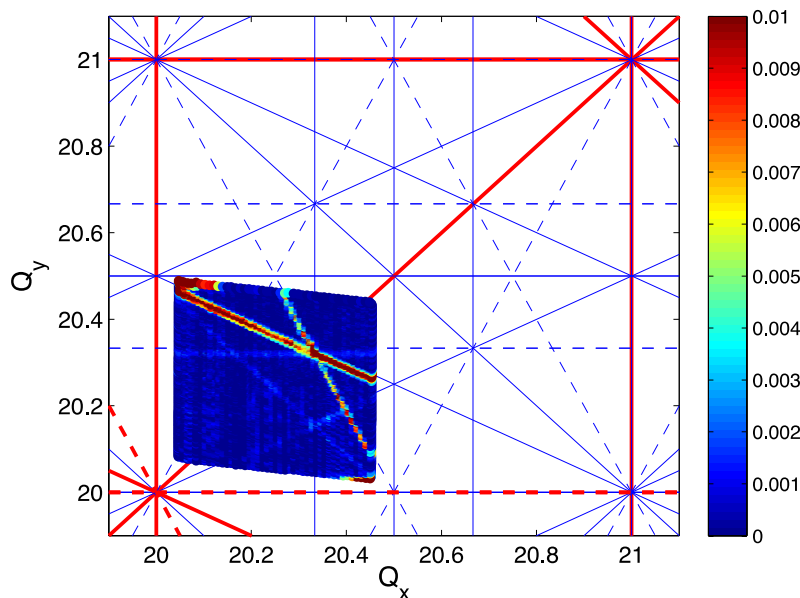
❑ **Resonances in the nominal optics**

- ❑ Normal sextupole resonance Qx+2Qy is the strongest

- ❑ Coupling resonance (diagonal, either Qx-Qy or some higher order of this), Qx-2Qy normal sextupole

- ❑ Skew sextupole resonance 2Qx+Qy weak compared to Q20 case

- ❑ Stop-band width of the vertical integer is stronger (predicted by simulations)



Low $\gamma_t$ optics



Nominal Optics

34
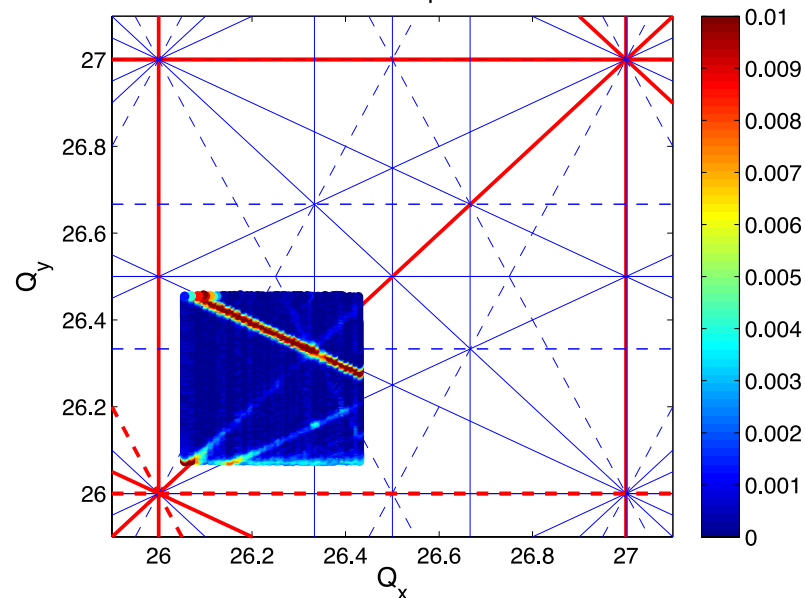
- Appearance of fixed points (periodic orbits) determine topology of the phase space

- Perturbation of unstable (hyperbolic points) opens the path to chaotic motion

- Resonance can overlap enabling the rapid diffusion of orbits

- Need numerical integration for understanding impact of non-linear effects on particle motion (dynamic aperture)

- Frequency map analysis is a powerful technique for analyzing particle motion in simulations but also in real accelerator experiments

1) A ring has super-periodicity of 4. Find a relationship for the integer tune that avoids systematic 3ʳᵈ and 4ᵗʰ order resonances. Generalize this for any super-periodicity.

2) Compute the tune-spread at leading order in perturbation theory for a periodic octupole perturbation in one plane.

3) Extend the previous approach to a general multi-pole.

4) Do skew multi-poles provide 1ˢᵗ order tune-shift with amplitude?